

1 **TITLE**

2 **Heme A synthesis and CcO activity are essential for *Trypanosoma cruzi* infectivity and**
3 **replication**

4

5

6 **AUTHORS**

7 Marcelo L. Merli*, Brenda A. Cirulli*, Simón M. Menéndez-Bravo* and Julia A. Cricco*^{†1}

8

9

10 *Instituto de Biología Molecular y Celular de Rosario (IBR), Consejo Nacional de
11 Investigaciones Científicas y Técnicas CONICET – Facultad de Ciencias Bioquímicas y
12 Farmacéuticas, Universidad Nacional de Rosario UNR. Suipacha 531, S2002LRK , Rosario,
13 Argentina.

14 [†]Área Biofísica, Departamento de Química Biológica, Facultad de Ciencias Bioquímicas y
15 Farmacéuticas, Universidad Nacional de Rosario UNR. Suipacha 531, S2002LRK, Rosario,
16 Argentina.

17

18

19 **CORRESPONDING AUTHOR**

20 ¹Julia A. Cricco, e-mail: cricco@ibr-conicet.gov.ar

21

22 **ABSTRACT**

23 *Trypanosoma cruzi*, the causative agent of Chagas disease, presents a complex life cycle
24 and adapts its metabolism to nutrients availability. Although *T. cruzi* is an aerobic
25 organism, it does not produce heme. This cofactor is acquired from the host, and is
26 distributed and inserted into different heme-proteins such as respiratory complexes in the
27 parasite mitochondrion. It has been proposed that *T. cruzi*'s energy metabolism relies on a
28 branched respiratory chain with a cytochrome *c* oxidase type *aa3* (CcO) as the main
29 terminal oxidase. Heme A, the cofactor for all eukaryotic CcO, is synthesized *via* two
30 sequential enzymatic reactions catalyzed by heme O synthase (HOS) and heme A synthase

31 (HAS). Previously, TcCox10 and TcCox15 were identified in *T. cruzi*. They presented HOS
32 and HAS activity, respectively, when were expressed in yeast. Here, we present the first
33 characterization of TcCox15 in *T. cruzi*, confirming its role as heme A synthase. It was
34 differentially detected in the different *T. cruzi* stages, being more abundant in the
35 replicative forms. This regulation could reflect the necessity of more heme A synthesis, and
36 therefore more CcO activity at the replicative stages. Over-expression of a non-funtional
37 mutant caused a reduction in heme A content. Moreover, our results clearly showed that
38 this hindrance in the heme A synthesis provoked a reduction on CcO activity and, in
39 consequence, an impairment on *T. cruzi* survival, proliferation and infectivity. These
40 evidences support that *T. cruzi* depends on the respiratory chain activity along its life cycle,
41 being CcO an essential terminal oxidase.

42

43

44 **SUMMARY STATEMENT**

45 *Trypanosoma cruzi* requires heme A as cofactor for the cytochrome *c* oxidase (CcO) of the
46 mitochondrial respiratory chain. The impairment of heme A synthesis negatively affects
47 parasite proliferation and infectivity, confirming its essentiality in the parasite life-cycle
48 stages.

49

50 **SHORT TITLE**

51 Heme A synthesis is essential for *Trypanosoma cruzi*

52

53 **KEYWORDS**

54 *Trypanosoma cruzi*, heme A synthase, heme A, cytochrome *c* oxidase, Chagas disease

55

56 **ABBREVIATIONS LIST**

57 CcO, cytochrome *c* oxidase; DAPI, 4',6-diamidino-2-phenylindole; DMEM, Dulbecco's
58 Modified Eagle Medium; FBS, Fetal Bovine Serum; GFP, green fluorescence protein; Glc,

59 Glucose; Gly–EtOH, Glycerol–Ethanol; HAS, heme A synthase; HOS, heme O synthase; LIT,
60 Liver Infusion Tryptose; MOI, multiplicity of infection; PBS, phosphate buffered saline; SC-
61 URA, synthetic complete medium lacking Uracile; TcCox15, *Trypanosoma cruzi* Cox15
62 protein; YP, yeast extract, peptone, wt, wild type.

63

64

65 INTRODUCTION

66 Heme (heme B) is an essential molecule for most aerobic organisms of all
67 kingdoms, and it is the prosthetic group of nearly all the heme-proteins including
68 hemoglobin, myoglobin, catalases, peroxidases and mitochondrial respiratory complexes
69 (1–3). It is synthesized *via* a well-defined pathway that is highly conserved through
70 evolution (2,4,5), where the last step – the insertion of ferrous iron into the
71 protoporphyrin IX ring - is catalized by ferrochelatase. Heme B can also be converted into
72 heme C or A, which contain different modifications in the protoporphyrin ring (2). Heme A,
73 B and C are cofactors in complexes II, III and IV of the respiratory chain as well as in
74 cytochrome *c*. Cytochromes *c* and *c1* are examples of heme-proteins that contain heme
75 covalently bound to its apo-protein partner through its vinyl side chains (heme C), and
76 different mechanisms and enzymes were described for this type of attachment (6). The
77 only known protein which has heme A as a cofactor is the cytochrome *c* oxidase (CcO) or
78 complex IV of the mitochondrial respiratory chain (3,7). Heme A is synthesized *via* two
79 sequential enzymatic reactions starting from heme B. In the first reaction, catalized by the
80 heme O synthase (HOS) or Cox10, a farnesyl group is transferred to the C-2 vinyl group of
81 heme B to form heme O. During the second reaction, the methyl substituent on pyrrole
82 ring D is oxidized to an aldehyde by the heme A synthase (HAS), or Cox15, to form heme A
83 (Figure 1). Sequence analyses and biochemical studies have revealed that these enzymes
84 are highly conserved among eukaryotes and are located in the mitochondrial inner
85 membrane (3,7,8).

86 Trypanosomatids belong to the narrow group of eukaryotic organisms that are not
87 capable of synthesizing heme and, to overcome this deficiency, they extract this cofactor
88 from their environment. The mentioned group includes several organisms that cause

89 significant human and animal diseases worldwide, among them species of *Trypanosoma*
90 and *Leishmania*. *Trypanosoma cruzi* causes Chagas disease, the most prevalent parasitic
91 disease in the Americas (4,9). It is estimated that about 6 to 7 million people are infected
92 worldwide, mostly in Latin America and southern states of USA, where Chagas disease is
93 considered endemic. Moreover, it is also becoming relevant in non-endemic regions due to
94 migrations and the absence of control in blood banks and organ transplantation
95 (<http://www.who.int/mediacentre/factsheets/fs340/en/>) (10). This organism has a
96 complex life cycle that alternates between two hosts, an invertebrate and a vertebrate,
97 and involves at least four different stages. In the insect vector, two distinct forms were
98 described: the epimastigote, which is the replicative form, and the metacyclic
99 trypomastigote, the infective and non-replicative form that once in the mammals' blood
100 stream can infect any nucleated cell. In the mammal host two stages are undoubtedly
101 described: the amastigote (intracellular and replicative) and the bloodstream
102 trypomastigote (infective and non-replicative) forms. The last one is derived from the
103 intracellular amastigotes and released into the blood stream (11). During the different life-
104 cycle stages, the parasite adapts its metabolism to the nutrient availability inside the
105 different hosts. It is postulated that *T. cruzi*'s energy metabolism relies on the respiratory
106 chain, at least in some stages of its life cycle (12–14). It has also been proposed that a
107 branched respiratory chain is functioning in the parasite mitochondrion, with a type *aa3*
108 CcO as its main terminal oxidase, and with a contribution to the total oxygen consumption
109 of a putative alternative oxidase, as found in *T. brucei* (TAO), and/or an oxidase containing
110 cytochrome *o* (15–17). However, other putative terminal oxidases were not identified in *T.*
111 *cruzi*, neither from its genome sequence (18), nor from proteomic analysis that reported
112 the presence of polypeptides belonging to mitochondrial complexes such as NADH
113 dehydrogenase, cytochrome *c1*, subunits of CcO, and ATP synthase complexes (19,20).

114 Although *T. cruzi* lacks the complete route for heme biosynthesis, several studies
115 have been demonstrated that it is essential for this parasite. It is capable of acquiring
116 heme from its hosts (21,22) and inserting it in different heme-proteins. Also, heme is
117 transported to the parasite mitochondrion where the cytochromes *c* and *c1* are assembled
118 by a mechanism not yet characterized (9), and heme A is synthesized and inserted into the
119 mitochondrial CcO. In our laboratory we identified two *T. cruzi* proteins, named TcCox10

120 and TcCox15, which presented hemo O synthase and heme A synthase activity,
121 respectively, when they were expressed in yeast (23). Nevertheless, up to date, there is no
122 evidence about the role of TcCox10 and TcCox15, and the heme A synthesis in *T. cruzi*.

123 In this work, we present the first characterization of TcCox15, the HAS enzyme,
124 along the different life-cycle stages of *T. cruzi*. We focus on TcCox15's relevance to *T.*
125 *cruzi*'s survival and infectivity analyzing the expression of different versions of the TcCox15
126 recombinant protein -mutants and tagged ones- along the different life-cycle stages. Our
127 results demonstrate that TcCox15 has heme A synthase activity in *T. cruzi*, and that heme
128 A synthesis, and consequently the CcO activity, is essential in epimastigotes growth,
129 trypomastigotes infectivity and amastigotes intracellular replication.

130

131 MATERIALS AND METHODS

132 **Reagents.** Dulbecco's Modified Eagle Medium (DMEM) was obtained from Life
133 Technologies, Fetal Bovine Serum (FBS) from Natocor SA (Córdoba, Argentina), and hemin
134 from Frontier Scientific (Logan, UT, USA). Hemin stock solution was prepared in 50% (v/v)
135 EtOH, 0.01 N NaOH at a concentration of 1 mM, fractionated and stored at -80 °C.

136 **Bacterial and yeast strains.** *Escherichia coli* strains used for cloning procedures were
137 grown at 37 °C in Luria Bertani medium, supplemented with either ampicillin (100 µg/ml)
138 or kanamycin (50 µg/ml). *Saccharomyces cerevisiae* cells were grown in either a rich YP
139 medium (1% yeast extract, 2% peptone) or a synthetic complete medium (SC) lacking
140 Uracile for plasmid selection (SC-URA). In both cases, 2% Glucose (Glc) or 3% Glycerol–2%
141 Ethanol (Gly–EtOH) were used as carbon sources. *S. cerevisiae* strains DY5113 (MATa *ade2-*
142 *1 his3-1,15 leu2-3,112 trp1Δ ura3-1*) and *cox15Δ* (DY5113 *cox15::KanMX4*, (23)) were used
143 for heterologous complementation assays. Yeast cells were transformed using the lithium
144 acetate method (24).

145 **Cell lines and parasites.** Vero cells (ATCC CCL-81, already available in our laboratory) were
146 maintained in DMEM supplemented with 0.15% (w/v) NaHCO₃, 100 U/ml penicillin, 100
147 µg/ml streptomycin and 10% heat inactivated FBS (DMEM-10%FBS) at 37 °C in a humid
148 atmosphere containing 5% CO₂. *T. cruzi* epimastigotes Dm28c strain were cultured in a
149 Liver Infusion Tryptose (LIT) medium supplemented with 10% heat inactivated FBS (LIT-

150 10%FBS) and 20 μ M hemin (25), at 28 °C. Metacyclic trypomastigotes were obtained by
151 spontaneous differentiation of epimastigotes at 28 °C and used to infect monolayered
152 Vero cells to obtain cell-derived trypomastigotes. After two rounds of infection, the
153 resulting cell-derived trypomastigotes were used to infect monolayered Vero cells at a
154 multiplicity of infection (MOI) of 10-30 to monitor the cell infection experiments, or the
155 development and replication of intracellular amastigotes. During *T. cruzi* infections,
156 monolayered Vero cells were incubated in DMEM-2%FBS (2% of heat inactivated FBS) at
157 37 °C in a humid atmosphere containing 5% CO₂.

158 ***In silico* analysis.** The protein sequences: TcCox15 (TCDM_06426, obtained from TriTrypDB
159 database, <http://tritrypdb.org/tritrypdb/> (26)), the *S. cerevisiae* ScCox15 (YER141W,
160 obtained from the *Saccharomyces* Genome Database <http://www.yeastgenome.org>), and
161 the *B. subtilis* CtaA (CAB11340.1, obtained from NCBI <http://www.ncbi.nlm.nih.gov>) were
162 used for the amino acids' multiple sequence alignments using the Clustal W and Clustal X
163 version 2.0 software (<http://www.ebi.ac.uk/Tools/msa/clustalw2>, (27)).

164 **Ethics statement.** All experiments were approved by the Comité Institucional para el
165 Cuidado y Uso de Animales de Laboratorio, Facultad de Ciencias Bioquímicas y
166 Farmacéuticas, Universidad Nacional de Rosario, Argentina (Institutional Committee of
167 Animal Care and Use of the School of Biochemical and Pharmaceutical Sciences, National
168 University of Rosario Argentina) and conducted according to specifications of the US
169 National Institutes of Health guidelines for the care and use of laboratory animals (File
170 number 935/2015).

171 **Polyclonal antibodies that recognize TcCox15.**

172 To obtain anti-TcCox15 antibodies, we used the P1TcCox15 peptide expressed as a GST-
173 fusion protein. Experimental details are included in the Supporting Information. The rabbit
174 polyclonal antibodies were obtained from the Animal Facility, Facultad de Ciencias
175 Bioquímicas y Farmacéuticas - Universidad Nacional de Rosario. Animals were housed and
176 maintained according to institutional guidelines.

177 **TcCox15.His-GFP fusion protein.** The *TcCOX15.HIS-GFP* recombinant gene was made in a
178 two-step procedure. First, the *TcCOX15.HIS* sequence was amplified by PCR, using the

179 pBluescriptIIKS(-).*TcCOX15.HIS* vector as a template (23), and FP_*TcCOX15* and RP_noStop
180 primers (Table S1) to eliminate STOP codon at its 3'-end; *Bam*HI and *Xho*I restriction sites
181 flanked the *TcCOX15.HIS-nonSTOP* sequence. Also the primers FP_*GFP* and RP_*GFP*, listed
182 in Table S1, were designed to amplify GFP sequence from a plasmid available in the
183 laboratory introducing the *Xho*I restriction site at the 5'-end and *Sal*I *Eco*RV *Xba*I at the 3'-
184 end. The GFP PCR product was treated with the *Xho*I and *Xba*I restriction enzymes and the
185 *TcCOX15.HIS-nonSTOP* was treated with *Bam*HI and *Xho*I enzymes. *TcCOX15.HIS-nonSTOP*
186 genes and the GFP gene were cloned together into a pENTRTM3C vector (Gateway system®,
187 Invitrogen) to form *TcCOX15.HIS-GFP*. The cloning procedure was verified by sequencing
188 the DNA insert. After that, *TcCOX15.HIS-GFP* was cloned in p426.M25 vector previously
189 used in our laboratory for yeast complementation assays (23) and in pTcINDEX vectors
190 (28) for *T. cruzi* expression assays.

191 ***TcCOX15.HIS* mutant genes.** The mutants *TcCOX15H129A*, *TcCOX15H206A* and
192 *TcCOX15H307A* were made following the site directed mutagenic method described by
193 Oded Edelheit with some modifications (29). The mutagenic primers are listed in Table S1.
194 The pENTR3C.*TcCOX15.HIS* vector obtained from *E. coli* DH5α (*dam*⁺) was used as a
195 template. The reaction mixture (100 μl) contained 0.3 mM of each dNTP, 0.2 μM of each
196 mutagenic primer, 400 ng of template DNA, 1 mM MgSO₄, 10 μl of the 10X buffer
197 (Invitrogen) and 2.5 units of *Pfx* Platinum DNA polymerase (Invitrogen). The reaction steps
198 were: one cycle of 3 minutes at 95 °C, then 18 cycles of 30 seconds at 95 °C, 1 minute at 55
199 °C and 5 minutes at 68 °C. After that, the PCR mix was treated with 20 U of *Dpn*I
200 (Fermentas) at 37 °C for 2 hours where the methylated DNA used as template was
201 completely digested. 10 μL of 1 M CaCl₂ were added to 90 μL of the mixture and then used
202 to transform *E. coli* DH5α cells by the chemical method. The plasmids containing the
203 mutated sequences were identified by restriction enzyme treatment since a specific
204 restriction site was introduced together with the aminoacid substitution by the mutagenic
205 primer (30). The mutations were confirmed by DNA sequencing, and the inserts cloned to
206 pTcINDEX vector (28) for *T. cruzi* expression assays and also between *Bam*HI and *Sal*I
207 restriction sites in p426.MET25 vector for yeast complementation assays (23).

208 **Spot growth assay.** *S. cerevisiae* wt and *cox15Δ* cells transformed with plasmids derived of
209 p426.MET25 were grown overnight in SC-URA medium at 30 °C with vigorous shaking.

210 Then, the cells were suspended at a final $D^{600} = 1$ and 5 μl of four serial dilutions (1:10 to
211 1:10000) plated in solid SC-URA Glc and SC-URA Gly-EtOH. When it was necessary, the
212 methionine concentration was modified to evaluate the effect caused by different amount
213 of overexpressed recombinant protein, since the *MET25* promoter is repressed by
214 methionine (31). The plates were incubated at 30 °C for 4–5 days.

215 **Parasites transfection.** *T. cruzi* epimastigotes Dm28c containing pLEW13 plasmid (28)
216 (Dm28c.pLEW13), were grown in LIT-10%FBS with 20 μM hemin plus 250 $\mu\text{g/ml}$ G418 to
217 approximately 3×10^7 cells/ml. Epimastigotes were collected by centrifugation at 3000 \times g
218 for 5 minutes, washed twice with PBS, and 1×10^8 cells were suspended in 0.35 ml of
219 electroporation buffer pH 7.5 (137 mM NaCl, 2.7 mM KCl, 4.7 mM Na_2HPO_4 , 1.47 mM
220 KH_2PO_4 , 0.5 mM MgCl_2 , 0.1 mM CaCl_2). The cells were transferred to a 0.2 cm gap cuvette
221 and 50 μl of 0.4 $\mu\text{g}/\mu\text{l}$ DNA was added (wt and mutant genes cloned into pTcINDEX
222 plasmid). The mixture was placed in ice for 15 min and subjected to 1 pulse of 450 V and
223 500 μF using GenePulser II (Bio-Rad, Hercules, USA). Then, it was transferred to 3 ml of LIT-
224 10%FBS with 20 μM hemin and incubated at 28 °C. 48 hours post electroporation 50 $\mu\text{g/ml}$
225 of Hygromycin B was added, and at 72 to 96 hours, the cultures were diluted and
226 Hygromycin B concentration was increased to 200 $\mu\text{g/ml}$. Stable resistant transfected cells
227 were obtained approximately 30-45 days post transfection.

228 **Epimastigotes' growth curves.** Epimastigotes transfected with pTcINDEX plasmids
229 containing the wt or mutant *TcCOX15* genes were maintained in LIT-10%FBS plus 20 μM
230 hemin. They were collected by centrifugation, and 5×10^6 cells were suspended in 1.5 ml
231 of fresh medium. After 24 hours of growth, tetracycline was added at different
232 concentrations (0.05, 0.15 and 0.25 $\mu\text{g/ml}$) to induce gene expression and the cultures
233 were maintained for 7-10 days in mid-log phase by periodic dilutions every two days. Cell
234 growth was monitored by cell counting in a Neubauer chamber. Samples were taken 3-4
235 days post induction to analyze protein expression by Western blot assay and indirect
236 immunofluorescence method, heme A levels by the heme pyridine hemochrome method,
237 and CcO activity by oxygen consumption rates measurement. In all cases, the accumulation
238 of the recombinant proteins caused by the addition of different amount of tetracycline
239 was evaluated by Western blot assay. Recently, it was reported by Moullan and col. that
240 tetracycline can disturb mitochondrial function in different eukaryotic models (32). On the

241 other hand, Hashimi and col. reported later that higher tetracycline concentrations did not
242 affect *T. brucei* and *L. tolerantoae* (33), but they did not test the effect on *T. cruzi* (32,33).
243 Considering the presented evidences, and to avoid other possible effects caused by the
244 mitochondrial protein imbalance, we performed the assays using the lower inductor
245 concentration that caused a phenotypic difference between the epimastigotes containing
246 the recombinant proteins (wt and mutants) and the controls.

247 **Cell infection assay using trypomastigotes overexpressing the recombinant *TcCOX15* wt**
248 **and mutant genes.** Cell-derived trypomastigotes (containing pTcINDEX,
249 pTcINDEX.*TcCOX15.HIS* and pTcINDEX.*TcCOX15H307A.HIS*) were used to infect
250 monolayered Vero cells to evaluate the effects of (wt and mutant) TcCox15 recombinat
251 protein during tripomastigotes' infection and intracellular amastigotes' replication (2-3
252 days post infection) as it was previously described (22,34). Briefly, the cell-derived
253 trypomastigotes were collected by centrifugation at 4,000 x g for 10 minutes and pre-
254 incubated in both, the absence (-) and the presence (+) of 0.20 µg/ml tetracycline for 1 h.
255 Then they were incubated during 16 hours with 3 x 10³ Vero cells plated on cover glasses
256 (maintained in DMEM-2%FBS at 37 °C in a humid atmosphere containing 5% CO₂) at a MOI
257 (multiplicity of infection) of 10-30 trypomastigotes/cell (Infection), Then, the monolayered
258 Vero cells were washed twice with PBS, the complete medium was renewed without (-) or
259 with (+) 0.20 µg/ml tetracycline and then incubated during 2 - 3 days (post infection). After
260 that, the treated monolayered cells were washed twice with PBS, fixed with methanol for
261 15 minutes, stained with Giemsa reagent and mounted with Canada Balsam (Biopack). To
262 quantify the percentage of infected cells and the number of amastigotes per infected cell,
263 200 cells per slide were analyzed by optical microscopy. All conditions were run by
264 triplicate (technical replicates) and the results are representative of at least two
265 independent assays (biological replicates).

266 **Yeast mitochondrial purification.** Intact yeast mitochondria were isolated from yeast
267 grown in a synthetic medium as previously described (23). The final pellet containing the
268 crude mitochondrial fraction was suspended in a Spheroplast buffer (0.6 M Manitol, 20
269 mM Tris:HCl pH 7.5, 1 mM PMSF), immediately used or fractioned and stored at -80 °C.

270 **Total protein cell extracts obtained from different life-cycles stages of *T. cruzi*.**
271 Epimastigotes maintained in exponential growth phase in LIT-10%FBS with 20 μ M hemin
272 (plus tetracycline in case of transfectant epimastigotes) were collected by centrifugation at
273 2000 x g, washed twice with PBS, and suspended in a Lysis buffer (8 M urea, 20 mM Hepes
274 pH 8). The cell-derived trypomastigotes were collected by centrifugation at 6000 x g for 10
275 minutes, washed twice with PBS, and suspended in the same Lysis buffer. Amastigotes
276 were obtained from infected monolayered Vero cells maintained in DMEM-2%FBS. 48
277 hours post infection, the monolayered cells were washed twice with cold PBS and lifted
278 with a cell scraper in 5 ml of PBS. The cells were collected by centrifugation at 1500 x g for
279 8 minutes and suspended with 1 ml of PBS, and then disrupted by a 27G syringe. The
280 amastigotes were collected by centrifugation at 1500 x g for 8 minutes and suspended in
281 Lysis buffer.

282 **Immunoblotting.** Total protein from *T. cruzi* cell-free extracts ($10\text{-}15 \times 10^6$ cells/well) or *S.*
283 *cerevisiae* mitochondrial fractions (30-50 μ g protein per well) were heated at 50 $^{\circ}$ C for 15
284 minutes in a loading buffer (1.8% SDS, 5% glycerol and 0.5% β -mercaptoethanol),
285 separated by electrophoresis on a 12-15% SDS-PAGE, and electrotransferred onto
286 nitrocellulose membranes (Amersham). The following antibodies were used for protein
287 detection: rabbit polyclonal anti-TcCox15 antibody, rabbit monoclonal anti-GFP antibody
288 (Santa Cruz Biotechnology), mouse monoclonal anti-His antibody (Calbiochem) or rabbit
289 polyclonal anti-6xHis HRP conjugated antidody (ABCAM), mouse monoclonal anti-
290 trypanosome α -tubulin clone TAT-1 antibody (a gift from K. Gull, University of Oxford,
291 England, United Kingdom), rabbit polyclonal anti-mitochondrial tryparedoxin peroxidase
292 antibody (anti-TcmPx, kindly provided by Sergio Guerrero, Universidad Nacional del Litoral,
293 Argentina) (35), and rabbit polyclonal anti- β subunit of F1 ATPase complex antibody (anti-
294 sub β F1, a kind gift from A. Tzagollof, Columbia University, USA). Bound antibodies were
295 detected with peroxidase-labeled anti-rabbit IgG (Calbiochem) or peroxidase-labeled anti-
296 mouse IgG (Calbiochem) and ECL Prime Western Blotting Detection kit (GE Healthceare).
297 When it was necessary, the membranes were stripped 30 minutes at 50 $^{\circ}$ C with Stripping
298 buffer (2% SDS, 100 mM β -mercaptoethanol, 62.5 mM Tris pH 8). The ImageJ software was
299 used for the quantitative analysis (36,37).

300 **Indirect immunofluorescence.** Epimastigotes maintained in an exponential growth phase
301 in LIT-10%FBS with 20 μ M hemin (plus the addition of tetracycline when necessary) were
302 collected and 10×10^6 cells were incubated with 1 μ M Mitotracker (Invitrogen) in 100 μ L of
303 PBS during 60 minutes at 28 °C. The cells were fixed with 4% (w/v) paraformaldehyde in
304 PBS at room temperature for 10 min and permeabilized with 0.1% Triton X-100 in PBS for
305 10 min. Then they were incubated first with rabbit anti-TcCox15 polyclonal antibody
306 diluted in Immunofluorescence Buffer (IB - 0.1% Tween 20, 150mM Tris pH 7.5 and
307 150mM NaCl) plus 1 % BSA, washed, and later incubated with anti-rabbit IgG FitC
308 conjugated (Jackson Immuno Research) diluted in the same IB and 1 μ M DAPI (4',6-
309 diamidine-2-phenylindole). The slides were mounted with VectaShield (Vector
310 Laboratories). Images were acquired with a confocal Nikon Eclipse TE-2000-E2 microscope
311 using Nikon EZ-C1 software. The ImageJ software was used to process the images (36,37).
312 The autofluorescent background was rectified and the deconvolution treatment was
313 applied to all images. The co-localization quantitative analysis was performed using the
314 Image J software; the estimated Pearson's correlation coefficient and Manders' overlap
315 coefficients are reported.

316 **Oxygen consumption measurements.** The oxygen consumption rates were quantified
317 using a Clark electrode connected to a 5300 Biological Oxygen Monitor (Yellow Springs
318 Instrument Co.) from the linear response as previously described (23). The yeast cells
319 grown overnight in SC-URA Glc were collected, washed, and suspended in 3% glycerol
320 (v/v). The measurements of oxygen consumption rate (O_2 nmoles consumed per minute
321 and D^{600}) were carried out in 3% glycerol (v/v) at 30 °C in a final volume of 2 ml. The
322 reaction was completely inhibited by the addition of azide (a few grains).

323 The oxygen consumption rate of transfected epimastigotes (O_2 nmoles consumed by 10^6
324 cells per minute) was measured following the protocol previously described by Vercesi and
325 col. (38) with minor modifications. Epimastigotes transfected with pTcINDEX containing
326 the *TcCOX15* genes (wt and mutants) were treated with tetracycline for 3-4 days, then
327 collected, washed with PBS, suspended at 50×10^6 cells/100 μ L in TSB-EGTA (125 mM
328 sucrose, 65 mM KCl, 10 mM Tris:HCl pH 7.5, 1 mM $MgCl_2$, 2.5 mM KH_2PO_4 , 333 μ M EGTA)
329 and kept in ice. 5 mM succinate and 50 μ M digitonin were added to each sample

330 immediately before the assay. The measurements of oxygen consumption were carried
331 out in TSB-EGTA plus 5 mM succinate at 28 °C in a final volume of 2 ml.

332 **Heme pyridine hemochrome method.** $2-4 \times 10^9$ cells of transfected epimastigotes were
333 collected after 3-4 days post induction with tetracycline, washed with PBS, and pulled
334 down by high-speed centrifugation discharging the supernatant. Total hemes were
335 extracted from the cell pellet by the acetone:HCl extraction method previously described
336 with minor modifications (39). Briefly, the cell pellet was washed with 1 ml of cold
337 acetone:water (80:20) and then mixed with 1 ml of acetone:HCl (4 vol acetone and 1.5 vol
338 1.5 M HCl) to extract heme A and B. Then, the sample was centrifuged and the
339 supernatant was kept in a separated tube. Hemes were extracted again from the pellet
340 with 0.5 ml of acetone:HCl. Then, both supernatants were combined and mixed with 1 ml
341 of ethyl ether and 0.25 ml of 1.5 M HCl to extract hemes from the acetone:HCl solution.
342 The last step (ether extraction) was repeated but the extraction was performed with 0.5
343 ml of ethyl ether and 0.125 ml of 1.5 M HCl. The ethyl ether fractions were combined and
344 washed with 0.8 ml of 0.5 M HCl, and with 0.8 ml of 3% (w/v) NaCl. After ethyl ether
345 evaporation, the extracted hemes were suspended with 500 μ L PBS and their
346 concentrations quantified from the reduced – oxidized differential spectrum as described
347 previously (22). The 557 nm from heme B and 588 nm from heme A absorbance peaks
348 were identified spectrum and heme B and heme A concentrations were quantified using
349 the molar extinction coefficient $23.98 \text{ mM}^{-1} \text{ cm}^{-1}$ and $25.02 \text{ mM}^{-1} \text{ cm}^{-1}$, respectively (39).

350 **Statistical analysis.** The results are expressed as mean \pm S.D. of three technical replicates
351 (technical replica) from one representative of three independent experiments (biological
352 replica) unless otherwise indicated. Statistically significant differences between groups (*P*)
353 were analyzed using GraphPad Prism version 6.0 as indicated in each assay.

354

355 **RESULTS**

356 **TcCox15 is detected in the different life-cycle stages of *Trypanosoma cruzi***

357 To study the role and relevance of TcCox15 in *T. cruzi*, first we evaluated its
358 presence along the parasite's life cycle. The endogenous protein was detected in all

359 assayed life-stages as shown in Figure 2, where anti-TcCox15 antibodies were used in the
360 Western blot assay. The replicative life-stages (epimastigotes and amastigotes) showed
361 higher TcCox15 levels than the infective and non-replicative stage (trypomastigotes). The
362 TcCox15 signal was normalized against tubulin or TcmPx, revealing the amount of this
363 protein was two times higher in epimastigotes than in amastigotes and five times higher
364 than in trypomastigotes (Figure 2B and C). These results suggest a major requirement for
365 HAS activity in the replicative stages.

366 **TcCox15 is detected in the mitochondrion of *Trypanosoma cruzi* epimastigotes.**

367 Indirect immunofluorescent assay on epimastigotes (Dm28c) were run to assess the
368 cellular localization of TcCox15 (using anti-TcCox15 antibodies), but the resulting
369 fluorescent signals presented very low intensity, impeding a clear identification of the
370 protein location. Alternatively, transfected epimastigotes containing the
371 pTcINDEX.*TcCOX15.HIS*, treated with tetracyclin during 3 days to induce the recombinant
372 gene expression, were analyzed. Anti-TcCox15 as the primary antibody and the anti-rabbit
373 FitC-conjugated as the secondary antibody allowed the detection of the recombinant
374 TcCox15.His. Also the samples were labeled with Mitotracker. In this case, the green
375 fluorescent signal corresponding to TcCox15.His overlapped with the Mitotracker's red
376 signal, as shown in Figure 2D, suggesting that TcCox15 localizes in the parasite's
377 mitochondrion, as it was expected.

378 **TcCOX15.His-GFP fusion is dominant negative**

379 In addition to TcCox15.His we also constructed a recombinant protein fused to a C-
380 terminal GFP where the *TcCOX15.HIS* gene was C-terminally tagged with a GFP sequence
381 generating the *TcCOX15.HIS-GFP* recombinant gene. The functionality of TcCox15.His-GFP
382 was evaluated in *cox15Δ* yeast cells. Then wt and *cox15Δ* yeast cells were transformed
383 with *TcCOX15.HIS-GFP* cloned in pRS426.MET25, and plated on selective media
384 supplemented with Glc or Gly-EtOH to test the respiratory capacity. The expression of
385 TcCoxX15.His-GFP did not fully restore the respiratory deficiency of the knocked out
386 *cox15Δ* cells as it is shown in Figure 3A. Moreover, the oxygen consumption of *cox15Δ* cells
387 over-expressing TcCox15.His-GFP was lower than cells expressing TcCox15.His (Figure 3B).
388 The presence of both recombinant proteins was corroborated by Western blot assays

389 using anti-TcCox15 and anti-GFP antibodies (Figure 3C), and also TcCox15.His-GFP was
390 visualized in the yeast cells by confocal microscopy (Figure 3D). Surprisingly, the over-
391 expression of the recombinant protein TcCox15.His-GFP, contrary to TcCox15.His, affected
392 negatively the respiratory growth of the wt cells (Figure 3E). Presumably, this dominant
393 negative effect was due to a defective formation of the complexes necessary for heme A
394 synthesis and/or heme A insertion into subunit I of CcO (40,41). In addition to this
395 evidence, *TcCOX15.HIS-GFP* was also cloned in pTcINDEX (28) and the resulting plasmid
396 used to transfect *T. cruzi* epimastigotes (Dm28c.pLEW13). It was not possible to obtain
397 transfectant epimastigotes harboring pTcINDEX.*TcCOX15.HIS-GFP*, consistently with the
398 phenotype observed when *TcCOX15.HIS-GFP* was expressed in wt yeast.

399 **The conserved histidine residues of TcCox15 enzyme are essential for heme A synthase** 400 **activity**

401 Several His residues were described as essential for the CtaA activity (*B. subtilis* HAS
402 enzyme), such as His60, His123, and His216 (42). These residues are conserved in TcCox15,
403 corresponding to His129, His206 and His307 following the TcCox15 numbering
404 (Supplementary Figure S1) (23). To analyze their relevance, each one was changed by Ala
405 generating the TcCox15HxxxA.His (H129A, H206A and H307A) mutant proteins (all of them
406 containing a C-terminal His-tag). The HAS activity of these recombinant proteins was
407 evaluated in yeast cells, then the *TcCOX15HxxxA.HIS* variants cloned in p426.MET25
408 (p426.MET25.*TcCOX15H129A.HIS*, p426.MET25.*TcCOX15H206.HIS* and
409 p426.MET25.*TcCOX15H307A.HIS*) were used to transform the *cox15Δ* cells as well as
410 p426.MET25 (negative control), and p426.MET25.*TcCOX15.HIS* and
411 p426.MET25.*ScCOX15.HIS* as positive controls (23). The presence of TcCox15H129A.His,
412 TcCox15H206A.His and TcCox15H307A.His did not allow the recovery of the respiratory
413 growth of *cox15Δ* cells, and also the recombinant strains did not exhibit any oxygen
414 consumption activity as it is shown in Figure 4A and B respectively. The presence of the wt
415 TcCox15.His and the TcCox15HxxxA.His mutants in mitochondrial fractions was verified by
416 Western blot assays (Figure 4C). In summary, the respiratory deficiency was not due to the
417 absence of these recombinant proteins in the yeast mitochondria but instead to the
418 mutations introduced in TcCox15 sequence. Also, the phenotype caused by the over-
419 expression of TcCox15HxxxA.His was evaluated in wt yeast cells and its growth was not

420 affected like it was observed with the over-expression of the TcCox15.His-GFP. This
421 suggests that TcCox15HxxxA.His mutants did not affect the activity of the native HAS
422 enzyme in yeast (*ScCox15*). These results show that the mutations introduced in the
423 *TcCOX15* gene affected the enzyme function without major effect on its assembly and
424 accumulation in the yeast mitochondria, which makes them promising candidates to
425 evaluate their function in the native organism, *T. cruzi*.

426 **The presence of TcCox15 mutant negatively affects heme A synthesis, CcO activity and** 427 **epimastigotes proliferation**

428 As an approach to analyze the role of TcCox15 in *T. cruzi*, *TcCOX15HxxxA.HIS* (H129,
429 H206 and H307) genes were cloned in pTcINDEX vector and pTcINDEX.*TcCOX15H129A.HIS*,
430 pTcINDEX.*TcCOX15H206A.HIS*, pTcINDEX.*TcCOX15H307A.HIS*, in addition to
431 pTcINDEX.*TcCOX15.HIS*, were used to transfect epimastigotes Dm28c.pLEW13 (28). We did
432 not succeed in obtaining epimastigotes transfected with pTcINDEX.*TcCOX15H206A.HIS*, so
433 we decided to exclude this mutant for the studies conducted afterwards. We tested the
434 phenotype caused by the induction of the recombinant genes (*TcCOX15.HIS* and
435 *TcCOX15HxxxA.HIS*) by the addition of different amounts of tetracycline, from 0 to 0.25
436 µg/ml. In this case, we did not observe any effects in the controls (epimastigotes harboring
437 pTcINDEX) up to 0.5 µg/ml of tetracycline (Figure 5A, B and C) and the induction of the wt
438 gene expression (*TcCOX15.HIS*) caused a mild negative effect on growth when the
439 concentration of tetracycline was increased from 0.15 to 0.25 µg/ml (Figure 5A). However,
440 the induction of both mutant genes severely impaired the epimastigotes' growth at the
441 lowest tetracycline concentration assayed (0.15 µg/ml) as shown in Figure 5B and C. The
442 effect produced by the presence of recombinant proteins was reported as a percentage of
443 parasite number of induced/non-induced conditions at the end of the growth curve, day 8
444 (Figure 5D). The accumulation of the recombinant proteins was validated by Western blot
445 assays (Figure 6A). Also, the cellular location of the mutant proteins (TcCox15H129A.His
446 and TcCox15H307A.His) was verified by indirect immunofluorescence assays (Figure 6B),
447 where the signal corresponding to the TcCox15HxxxA.His overlapped the mitochondrial
448 marker signal (Mitotracker), similarly to TcCox15 wt (Figure 2D), suggesting that the
449 mutations (H129A and H307A) did not affect the protein localization.

450 Afterwards, heme A synthesis and CcO activity were evaluated on epimastigotes
451 over-expressing TcCox15.His and TcCox15H307A.His recombinant proteins. Heme A
452 content was quantified by the pyridine hemochrome method (39) and CcO activity by
453 oxygen consumption measurements. The heme A content is reported in Table 1. All the
454 samples showed similar heme B concentrations, however, epimastigotes containing the
455 TcCox15H307A.His non-functional enzyme showed a 50% reduction in heme A
456 concentration, which is also denoted by the heme A/heme B ratio. Moreover, the parasites
457 containing the TcCox15H307A.His decreased about 40-45% the oxygen consumption rates
458 when compared to the non-induced samples (Figure 7). Conversely, parasites containing
459 TcCox15.His (wt protein) did not show any significant variations in the oxygen
460 consumption rates (Figure 7). Taking into account all results presented here, we can
461 postulate that the over-expression of the non-functional TcCox15 mutants caused a
462 negative effect over heme A synthesis, affecting the function of the CcO complex and
463 epimastigotes' proliferation.

464 **The presence of the TcCox15 non-functional mutant negatively affects *T. cruzi* infection**
465 **(trypomastigotes) and intracellular replication (amastigotes)**

466 We evaluated if any reduction in heme A synthesis and consequently CcO activity
467 could affect *T. cruzi* infection and intracellular replication. Cell-derived trypomastigotes
468 containing pTcINDEX, pTcINDEX.*TcCOX15.HIS* and pTcINDEX.*TcCOX15H307A.HIS* plasmids
469 pre-treated without or with 0.20 µg/ml of tetracycline, were incubated with monolayered
470 Vero cells at a ratio of 10 trypomastigotes/cell during 16 h at 37°C without or with the
471 addition of tetracycline (infection without (-), Infection with (+)). Then, the free
472 trypomastigotes were washed out, the complete medium was replaced without (-) or with
473 (+) the addition of 0.20 µg/ml of tetracycline and the cells incubated for another 2 days,
474 (post infection without (-), post infection with (+)). Then, the cells were stained with
475 Giemsa, and the number of infected cells and the intracellular amastigotes per infected
476 cells were evaluated microscopically. No effect was observed in parasites transfected with
477 the pTcINDEX (not shown). The presence of the recombinant TcCox15.His (wt enzyme) did
478 not affect the number of infected cells or the intracellular amastigotes per infected cells at
479 any of the assayed conditions, as shown in Figures 8A and B. Representative Giemsa
480 stained cells infected with *T. cruzi* expressing TcCox15.His are presented in Figure 8C. On

481 the other hand, the expression of TcCox15H307A.His impacted negatively on the number
482 of infected cells and the amount of amastigotes per infected cell (Figure 8D and E).
483 Induction of *TcCOX15H307A.HIS* expression during infection (+/- or +/+) caused a reduction
484 in the number of infected cells by approximately 50%, but no effect was observed when
485 the tetracycline had been added once the infection was established (-/+) (Figure 8D). Also,
486 a significant reduction in the number of amastigotes per infected cell was caused when the
487 tetracycline was added during the infection (+/-) or when it was maintained throughout
488 the whole assay (+/+). Additionally, a lower number of amastigotes per infected cell was
489 observed when tetracycline was added once the infection was established (-/+), but the
490 effect was less severe (Figure 8E). A representative picture of infected cells with *T. cruzi*
491 over-expressing TcCox15H307A.His is presented in Figure 8F. Both recombinant proteins
492 (TcCox15.His and TcCox15H307A.His) were detected by Western blot assay from total cell-
493 free extracts of transfected trypomastigotes and amastigotes (Figure 8G). We also verified
494 that the impairment in heme A synthesis affected the earlier steps on the infection
495 processes, as it is described in supporting information, where the over-expression of
496 TcCox15H307A.His recombinant protein caused a reduction on the percentage of infected
497 cells at short periods of time post infection (Figure S4). Thus, the presence of the TcCox15
498 non-functional mutant that reduces the heme A synthesis impaired the trypomastigote
499 infection and the intracellular amastigote replication.

500

501 **DISCUSSION**

502 Heme A is an essential cofactor produced only for the mitochondrial respiratory
503 complex IV (CcO); its insertion into subunit I of this complex is one of the first stages in the
504 CcO assembly (43). It is reported that the impairment in heme A synthesis and/or its
505 proper insertion into subunit I causes the proteolysis of the core of CcO in yeast, resulting
506 in a failure to detect this complex in the mitochondrial inner membrane (3). Therefore, a
507 lack of success in the synthesis and correct loading of heme A leads to respiratory chain
508 defects. *T. cruzi*, like other trypanosomatids relevant for human health, are aerobic
509 organisms that rely, at least in some of their life-cycle stages, on the mitochondrial
510 respiratory chain activity. Acknowledging these pieces of evidence, we postulate that

511 heme A might be synthesized according to the requirements of assembled and active CcO,
512 depending on the energetic metabolism of the *T. cruzi* life-cycle stages, nutrient
513 availability, or both. Furthermore, it seems reasonable that a reduction, or inhibition, in
514 heme A synthesis would render a defect on CcO activity that could lead to an increase in
515 the other terminal oxidase activities to compensate the impairment of the CcO function.

516 In this work, we present the first characterization of the TcCox15 enzyme (HAS) and
517 its product –heme A- in the native organism, *T. cruzi*. Our data indicates that TcCox15
518 should localize in the parasite mitochondrion, like all the eukaryotic HAS studied to date.
519 Recently reported transcriptomic analysis described that genes belonging to the Krebs
520 cycle, the respiratory chain and oxidative phosphorylation were significantly up-regulated
521 in epimastigotes, however, expression of genes related to respiration were detected in all
522 stages (44). Our results show that the expression of TcCox15 is regulated throughout the
523 parasite life cycle, being more abundant in the replicative stages (epimastigotes and
524 amastigotes) than in the infective stage (trypomastigotes), in agreement with the
525 transcriptomic analysis. Moreover, the TcCox15 expression pattern could reflect the
526 necessity of more respiratory chain activity during the replicative stages and to support
527 this demand of CcO, more HAS activity is required.

528 Several His residues, reported as essential for HAS activity in other organisms, are
529 conserved in the *T. cruzi* protein (23,42). Their replacement by Ala in TcCox15 rendered
530 non-functional enzymes (TcCox15H129A, TcCox15H206A and TcCox15H307A), and
531 together with the data reported from CtaA (*B. subtilis* HAS enzyme) (42), and recently from
532 ScCox15 (*S. cerevisiae* Cox15 enzyme) (41), it confirmed the relevance of the conserved His
533 residues in HAS activity. Also, the dominant negative effect observed when the
534 recombinant protein TcCox15.His-GFP was expressed in wt yeast cells, as well as the
535 inability to obtain transfected epimastigotes expressing this recombinant protein, suggests
536 that the presence of the C-terminal GFP interferes with HAS activity. This strongly supports
537 that TcCox15 could form relevant oligomeric complexes involved in heme A synthesis
538 and/or heme A insertion into subunit I of CcO as it was described for other eukaryotic HAS
539 (40,41). All these evidences indicate that heme A synthesis (at least the reaction catalized
540 by HAS), and possibly the cofactor insertion into CcO, are conserved in *T. cruzi* despite the
541 evolutionary divergence of this organism.

542 The non-functional mutants of TcCox15 arise as a useful tool to analyze the role of
543 heme A and its synthesis in *T. cruzi*. Their expression in epimastigotes, which also contain
544 endogenous TcCox15, negatively affects parasite growth as a direct consequence of the
545 impairment of heme A synthesis and consequently CcO activity. *A priori*, we exclude any
546 other possibility since the over-expression of the recombinant wt enzyme did not affect
547 heme A synthesis, CcO activity and epimastigotes' growth. Besides, these recombinant
548 proteins (wt and mutants) were localized in the parasite mitochondrion and interestingly
549 their presence did not affect heme B concentration in epimastigotes. Recently, it was
550 postulated that yeast Cox15 (ScCox15) associates with the CcO assembly intermediates
551 during Cox1 maturation, where Cox15 itself plays a relevant role in heme A insertion into
552 Cox1 (40,41). Then, it is reasonable to postulate that non-functional TcCox15 caused a
553 dominant-negative effect on epimastigotes' growth, where the inactive enzyme could
554 replace some of the endogenous TcCox15, disrupting the relevant complexes involved in
555 heme A synthesis and/or heme A insertion into CcO. In spite of the negative effects caused
556 in CcO activity by the presence of the TcCox15 non-functional mutants, the epimastigotes'
557 oxygen consumption rates were not compensated by any other mechanism under our
558 assay conditions. Therefore, our results confirm that CcO is the main terminal oxidase
559 essential for the epimastigotes' proliferation.

560 The expression of the recombinant non-functional HAS (TcCox15H307A.His)
561 negatively affected the cell line infection produced by trypomastigotes, while the
562 recombinant wt protein did not cause any effect. Notably, the endogenous level of
563 TcCox15 in trypomastigotes (infective form) was the lowest detected compared to the
564 replicative forms. Then, any small amount of a recombinant protein (wt or non-functional
565 mutant) could produce a serious imbalance in the HAS activity and finally in the amount of
566 fully assembled CcO. It has been previously proposed that once the trypomastigotes enter
567 the cell they have to differentiate into amastigotes and escape from parasitophorous
568 vacuole to establish the infection (45), or leave the cell (46,47). Interestingly, our results
569 demonstrate that heme A synthesis and CcO activity are essential for the cellular infection
570 produced by the *T. cruzi* trypomastigotes, and supports the idea that the trypomastigotes
571 attachment to mammalian cells is an active process that requires energy and
572 mitochondrial respiratory chain activity as it was previously described (48).

573 On the other hand, larger amounts of endogenous TcCox15 detected in the
574 epimastigotes and amastigotes forms are consistent with the hypothesis that the
575 replicative life-stages have a higher energy requirement than the infective stage. In
576 consequence, the parasite would need a fully active respiratory chain, with a concomitant
577 augmentation of heme A synthesis to assemble a higher amount of CcO complex. These
578 concepts are supported by the over-expression of the recombinant non-functional
579 TcCox15 that also impairs the intracellular replication of amastigotes. Likewise, this
580 evidence confirms that heme A synthesis and CcO activity are essential for amastigote
581 intracellular replication.

582 In summary, we have demonstrated that TcCox15 plays the role of heme A
583 synthase in *T. cruzi*. Despite the possible existence of a branched respiratory chain, our
584 results clearly show that CcO type *aa3* is the main terminal oxidase in all of *T. cruzi* life-
585 cycle stages and that its activity is essential for parasite growth and infection. Remarkably,
586 the data presented here demonstrate by the first time that impairment in CcO activity
587 (inhibiting its heme A synthesis) negatively affects, not only the replicative stages, but the
588 trypomastigotes infectivity. These evidences reinforce the idea of parasite energy
589 metabolism as an attractive therapeutic target to control infection and transmission.

590

591 **ACKNOWLEDGEMENTS**

592 We thank Professor Paul Cobine (Auburn University) for the critical reading of this
593 manuscript, Rodrigo Vena for the assistance in the acquisition of the confocal microscopy
594 images and Dolores Campos for her assistance in cell culture.

595

596

597 **DECLARATIONS OF INTEREST**

598 The authors have declared that no competing interests exist.

599

600

601 **FUNDING INFORMATION**

602 This work was supported by CONICET (National Research Council of Science and
603 Technology) [grant number PIP 2013-2015 0667 to JAC], and ANPCyT (National Agency of
604 Scientific and Technological Promotion) [grant number PICT 2010-2012 1992 to JAC].

605

606 **AUTHOR CONTRIBUTION STATEMENT**

607 JAC and MLM conceived, designed and supervised the project, MLM performed most of
608 designed experiments, BAC performed Western blot assays, SMM-B and JAC designed the
609 strategy to obtain the anti-TcCox15 antibodies. JAC, MLM, BAC and SMM-B discussed the
610 results. JAC and MLM wrote the manuscript with contributions from all other authors.

611

612 **REFERENCES**

- 613 1. Munro AW, Girvan HM, McLean KJ, Cheesman MR, Leys D. Heme and
614 Hemoproteins. In: Warren MJ, Smith AG, editors. Tetrapyrroles: birth, life and
615 death. Austin, TX: Landes Bioscience and Springer Science+Business Media, LLC;
616 2009. p. 160–83.
- 617 2. Hamza I, Dailey HA. One ring to rule them all: Trafficking of heme and heme
618 synthesis intermediates in the metazoans. *Biochim Biophys Acta - Mol Cell Res.*
619 Elsevier B.V.; 2012;1823(9):1617–32.
- 620 3. Moraes CT, Diaz F, Barrientos A. Defects in the biosynthesis of mitochondrial heme c
621 and heme a in yeast and mammals. *Biochim Biophys Acta - Bioenerg.* 2004;1659(2–
622 3):153–9.
- 623 4. Kořený L, Lukeš J, Oborník M. Evolution of the haem synthetic pathway in
624 kinetoplastid flagellates: An essential pathway that is not essential after all? *Int J*
625 *Parasitol.* 2010;40(2):149–56.
- 626 5. Panek H, O’Brian MR. A whole genome view of prokaryotic haem biosynthesis.
627 *Microbiology.* 2002;148(8):2273–82.

- 628 6. Mavridou DA, I, Ferguson SJ, Stevens JM. Cytochrome *c* assembly. *IUBMB Life*.
629 2013;65(3):209–16.
- 630 7. Hederstedt L. Heme A biosynthesis. *Biochim Biophys Acta - Bioenerg* [Internet].
631 Elsevier B.V.; 2012;1817(6):920–7.
- 632 8. Barros MH, Tzagoloff A. Regulation of the heme A biosynthetic pathway in
633 *Saccharomyces cerevisiae*. *FEBS Lett*. 2002;516(1–3):119–23.
- 634 9. Tripodi KEJ, Menendez Bravo SM, Cricco JA. Role of heme and heme-proteins in
635 trypanosomatid essential metabolic pathways. *Enzyme Res*. 2011;2011:873230.
- 636 10. Coura JR, Vinas PA. Chagas disease: a new worldwide challenge. *Nature*. England;
637 2010;465(7301):S6-7.
- 638 11. Tyler KM, Engman DM. The life cycle of *Trypanosoma cruzi* revisited. *Int J Parasitol*.
639 2001;31(5–6):472–81.
- 640 12. Tielens AGM, van Hellemond JJ. Surprising variety in energy metabolism within
641 *Trypanosomatidae*. *Trends Parasitol*. 2009;25(10):482–90.
- 642 13. Cazzulo JJ. Intermediate metabolism in *Trypanosoma cruzi*. *J Bioenerg Biomembr*.
643 United States; 1994 Apr;26(2):157–65.
- 644 14. Bringaud F, Rivière L, Coustou V. Energy metabolism of trypanosomatids:
645 Adaptation to available carbon sources. *Mol Biochem Parasitol*. 2006;149(1):1–9.
- 646 15. Affranchino JL, Schwarcz de Tarlovsky MN, Stoppani a O. Terminal oxidases in the
647 trypanosomatid *Trypanosoma cruzi*. *Comp Biochem Physiol B*. 1986;85(2):381–8.
- 648 16. Silva TM, Peloso EF, Vitor SC, Ribeiro LHG, Gadelha FR. O₂ consumption rates
649 along the growth curve: new insights into *Trypanosoma cruzi* mitochondrial
650 respiratory chain. *J Bioenerg Biomembr*. 2011;43(4):409–17.
- 651 17. Chaudhuri M, Ott RD, Hill GC. Trypanosome alternative oxidase: from molecule to
652 function. *Trends Parasitol*. 2006;22(10):484–91.
- 653 18. El-Sayed NM, Myler PJ, Bartholomeu DC, Nilsson D, Aggarwal G, Tran A-N, et al. The

- 654 genome sequence of *Trypanosoma cruzi*, etiologic agent of Chagas disease. *Science*.
655 2005;309(5733):409–15.
- 656 19. Parodi-Talice A, Monteiro-Goes V, Arrambide N, Avila AR, Duran R, Correa A, et al.
657 Proteomic analysis of metacyclic trypomastigotes undergoing *Trypanosoma cruzi*
658 metacyclogenesis. *J MASS Spectrom*. 2007;42:1422–1432.
- 659 20. Ferella M, Nilsson D, Darban H, Rodrigues C, Bontempi EJ, Docampo R, et al.
660 Proteomics in *Trypanosoma cruzi*- Localization of novel proteins to various
661 organelles. *Proteomics*. 2008;8(13):2735–49.
- 662 21. Cupello MP, Souza CF De, Buchensky C, Soares JBRC, Laranja GAT, Coelho MGP, et
663 al. The heme uptake process in *Trypanosoma cruzi* epimastigotes is inhibited by
664 heme analogues and by inhibitors of ABC transporters. *Acta Trop*. Elsevier B.V.;
665 2011;120(3):211–8.
- 666 22. Merli ML, Pagura L, Hernández J, Barisón MJ, Pral MF, Silber AM, et al. The
667 *Trypanosoma cruzi* Protein TcHTE Is Critical for Heme Uptake. *PLoS Negl Trop Dis*.
668 2016;1–18.
- 669 23. Buchensky C, Almirón P, Mantilla BS, Silber AM, Cricco JA. The *Trypanosoma cruzi*
670 proteins TcCox10 and TcCox15 catalyze the formation of heme A in the yeast
671 *Saccharomyces cerevisiae*. *FEMS Microbiol Lett*. 2010;312(2):133–41.
- 672 24. Gietz RD, Woods RA. Transformation of yeast by lithium acetate/single-stranded
673 carrier DNA/polyethylene glycol method. *Methods Enzymol*. United States;
674 2002;350:87–96.
- 675 25. Camargo EP. Growth and differentiation in *trypanosoma cruzi*. I. Origin of metacyclic
676 trypanosomes in liquid media. *Rev Inst Med Trop Sao Paulo*. BRAZIL; 1964;6:93–100.
- 677 26. Aslett M, Aurrecochea C, Berriman M, Brestelli J, Brunk BP, Carrington M, et al.
678 TriTrypDB: A functional genomic resource for the Trypanosomatidae. *Nucleic Acids*
679 *Res*. 2009;38(SUPPL.1):457–62.
- 680 27. Larkin M a., Blackshields G, Brown NP, Chenna R, Mcgettigan P a., McWilliam H, et
681 al. Clustal W and Clustal X version 2.0. *Bioinformatics*. 2007;23(21):2947–8.

- 682 28. Taylor MC, Kelly JM. pTcINDEX: a stable tetracycline-regulated expression vector for
683 Trypanosoma cruzi. BMC Biotechnol. 2006;6(32).
- 684 29. Edelheit O, Hanukoglu A, Hanukoglu I. Simple and efficient site-directed
685 mutagenesis using two single-primer reactions in parallel to generate mutants for
686 protein structure-function studies. BMC Biotechnol. 2009;9:61.
- 687 30. Sambrook, Joseph and Fritsch, Edward F and Maniatis T and others. Molecular
688 Cloning: A Laboratory Manual. Cold Spring Harbor Laboratory press New York; 1989.
- 689 31. Mumberg D, Muller R, Funk M. Regulatable promoters of Saccharomyces cerevisiae:
690 comparison of transcriptional activity and their use for heterologous expression.
691 Nucleic Acids Res. 1994;22(25):5767–8.
- 692 32. Moullan N, Mouchiroud L, Wang X, Ryu D, Williams EG, Mottis A, et al. Tetracyclines
693 disturb mitochondrial function across eukaryotic models: A call for caution in
694 biomedical research. Cell Rep. 2015;10(10):1681–91.
- 695 33. Hashimi H, Kaltenbrunner S, Zíková A, Luke J. Trypanosome Mitochondrial
696 Translation and Tetracycline : No Sweat about Tet. PLoS Pathog. 2016;12(4):1–5.
- 697 34. Ritagliati C, Villanova GV, Alonso VL, Zuma AA, Cribb P, Motta MCM, et al.
698 Glycosomal bromodomain factor 1 from Trypanosoma cruzi enhances
699 trypomastigote cell infection and intracellular amastigote growth. Biochem J.
700 2016;473(1):73–85.
- 701 35. Nogueira FB, Ruiz JC, Robello C, Romanha AJ, Murta SMF. Molecular
702 characterization of cytosolic and mitochondrial tryparedoxin peroxidase in
703 Trypanosoma cruzi populations susceptible and resistant to benznidazole. Parasitol
704 Res. 2009;104(4):835–44.
- 705 36. Rasband WS. ImageJ. U S Natl Institutes Heal Bethesda, Maryland, USA.
- 706 37. Schneider C a, Rasband WS, Eliceiri KW. NIH Image to ImageJ: 25 years of image
707 analysis. Nat Methods. Nature Publishing Group; 2012;9(7):671–5.
- 708 38. Vercesi AE, Bernardes CF, Hoffmann ME, Gadelha FR, Docampo R. Digitonin

- 709 permeabilization does not affect mitochondrial function and allows the
710 determination of the mitochondrial membrane potential of *Trypanosoma cruzi* in
711 Situ. *J Biol Chem.* 1991;266(22):14431–4.
- 712 39. Berry EA, Trumpower BL. Simultaneous determination of hemes a, b, and c from
713 pyridine hemochrome spectra. *Anal Biochem.* 1987;161(1):1–15.
- 714 40. Bareth B, Dennerlein S, Mick DU, Nikolov M, Urlaub H, Rehling P. The heme a
715 synthase Cox15 associates with cytochrome c oxidase assembly intermediates
716 during Cox1 maturation. *Mol Cell Biol.* 2013;33(20):4128–37.
- 717 41. Swenson S, Cannon A, Harris NJ, Taylor NG, Fox JL, Khalimonchuk O. Analysis of
718 Oligomerization Properties of Heme a Synthase Provides Insights into its Function in
719 Eukaryotes. *J Biol Chem.* 2016 Mar 3;291(19):10411–25.
- 720 42. Hederstedt L, Lewin A, Throne-Holst M. Heme A synthase enzyme functions
721 dissected by mutagenesis of *Bacillus subtilis* CtaA. *J Bacteriol.* 2005;187(24):8361–9.
- 722 43. Khalimonchuk O, Bestwick M, Meunier B, Watts TC, Winge DR. Formation of the
723 redox cofactor centers during Cox1 maturation in yeast cytochrome oxidase. *Mol*
724 *Cell Biol.* United States; 2010 Feb;30(4):1004–17.
- 725 44. Berná L, Chiribao ML, Greif G, Rodriguez M, Alvarez-Valin F, Robello C.
726 Transcriptomic analysis reveals metabolic switches and surface remodeling as key
727 processes for stage transition in *Trypanosoma cruzi*. *PeerJ.* 2017;5:e3017.
- 728 45. Fernandes MC, Andrews NW. Host cell invasion by *Trypanosoma cruzi*: A unique
729 strategy that promotes persistence. *FEMS Microbiol Rev.* 2012;36(3):734–47.
- 730 46. Andrade LO, Andrews NW. Lysosomal Fusion Is Essential for the Retention of
731 *Trypanosoma cruzi* Inside Host Cells. *J Exp Med.* 2004;200(9):1135–43.
- 732 47. Woolsey AM, Burleigh BA. Host cell actin polymerization is required for cellular
733 retention of *Trypanosoma cruzi* and early association with endosomal/lysosomal
734 compartments. *Cell Microbiol.* 2004;6(9):829–38.
- 735 48. Schenkman S, Robbins ES, Nussenzweig V. Attachment of *Trypanosoma cruzi* to

736 mammalian cells requires parasite energy, and invasion can be independent of the
 737 target cell cytoskeleton. Infect Immun. 1991;59(2):645–54.

738

739

740 **TABLE 1**

741

	heme A nmoles/ 1.10 ⁹ cells ± S.D.	heme B nmoles/ 1.10 ⁹ cells ± S.D.	heme A/heme B ± S.D.
vector	0.036 ± 0.005	1.225 ± 0.046	0.030 ± 0.003
TcCox15 + Tet	0.033 ± 0.003	1.477 ± 0.076	0.022 ± 0.001*
H307A + Tet	0.0160 ± 0.0003 *	1,207 ± 0.002	0.0136 ± 0.0003 **

742 **Table 1. The expression of recombinant TcCox15H307A.His enzyme decreases the**
 743 **amount of heme A in *T. cruzi* epimastigotes.** Heme content of epimastigotes transfected
 744 with pTcINDEX (vector), pTcINDEX.*TcCOX15.HIS* (TcCox15) or pTcINDEX.*TcCOX15H307A.HIS*
 745 (H307A) treated with 0.15 µg/mL tetracycline for 3 days was quantified by heme pyridine
 746 hemochrome method. The concentration of heme B and heme A were estimated from the
 747 reduced minus oxidized spectra, using the molar extinction coefficient 23.98 mM⁻¹ cm⁻¹
 748 (557 nm) and 25.02 mM⁻¹ cm⁻¹ (588 nm) respectively (39). Data are expressed as means ±
 749 S.D. of three technical replicates from one representative of at least three independent
 750 experiments (biological replica). Asterisks indicate a statistically significant difference
 751 compared to control, parasites transfected with pTcINDEX, **P* < 0.05 and ***P* < 0.01 (one-
 752 way analysis of variance followed by Tukey's Multiple Comparison post-test).

753

754

755 **FIGURES LEGENDS**

756 **Figure 1: Schematic representation of heme A synthesis.** Heme O Synthase (HOS) and
757 Heme A Synthase (HAS) (7).

758

759

760 **Figure 2. TcCox15 is detected in *T. cruzi* extracts from the different life-cycle stages.** (A)
761 Equal amounts of total cell-free extracts of epimastigotes (E), cell-derived trypomastigotes
762 (T), and amastigotes (A) were separated by SDS-PAGE, transferred to nitrocellulose, and
763 analyzed with anti-TcCox15, anti-tubulin as a loading control of total cell extract, and anti-
764 mitochondrial trypanredoxin peroxidase (anti-TcmPx) as a loading control as well as
765 mitochondrial marker. The Western blot is a representative from three independent
766 biological replicas. The relative amount of TcCox15 was quantified and normalized to anti-
767 tubulin (B) and anti-TcmPx intensity (C). Data are expressed as means \pm S.D. of three
768 independent assays. (D) Immunofluorescence assay of *T. cruzi* epimastigotes transfected with
769 pTcINDEX.*TcCOX15.HIS* incubated with 0.15 μ g/mL tetracycline for 3 days. TcCox15
770 (endogenous and recombinant proteins) was detected using anti-TcCox15 and FITC-
771 conjugated anti-rabbit (green) as secondary antibody. DNA was stained with DAPI (blue)
772 and mitochondrion was stained with Mitotracker (MT). DIC, differential interference
773 contrast image. The confocal images are a representative of multiple fields from three
774 different experiments. The colocalization analysis (Red:Green) was performed (Pearson's
775 correlation coefficient: 0.972, and Manders overlap coefficients: 0.895 and 0.924).

776

777

778 **Figure 3. The C-terminal GFP fusion to TcCox15 affects the heme A synthesis in yeast**
779 **cells.** (A) Spot growth assay of *cox15* Δ yeast cells transformed with p426.MET25 (vector),
780 p426.MET25.*TcCOX15.HIS* (TcCox15.His), p426.MET25.*TcCOX15.HIS-GFP* (TcCox15.His-GFP)
781 or p426.MET25.*ScCOX15.HIS* (ScCox15). 5 μ l of four serial dilutions from an initial cultures
782 of $D^{600}=1$ were plated on SC-URA Glc or SC-URA Gly-EtOH to test the respiratory capacity.

783 (B) The oxygen consumption rate of the same yeast cells was measured in 3% glycerol
784 (v/v). Data are expressed as means \pm S.D. of three technical replicates from one
785 experiment representative of three independent biological replicas. (C) Western blot of
786 mitochondrial extracts from *S. cerevisiae cox15* Δ cells transformed with
787 p426.MET25.*TcCOX15.HIS* (TcCox15.His) or p426.MET25.*TcCOX15.HIS-GFP* (TcCox15.His-
788 GFP), grown in SC-URA 0.2% Glucose, 1.8% Galactose, using the following antibodies: anti-
789 TcCox15, and anti- β subunit of F1 complex (anti-sub β F1) as a loading control of yeast
790 mitochondrial extract. (D) Confocal microscopy images of *S. cerevisiae cox15* Δ cells
791 transformed with p426.MET25.*TcCOX15.GFP* incubated overnight in SC-URA Gly-EtOH. (E)
792 Spot growth assay of WT yeast cells transformed with p426.MET25.*TcCOX15.HIS*
793 (TcCox15.His) or p426.MET25.*TcCOX15.HIS-GFP* (TcCox15.His-GFP). 5 μ l of four serial
794 dilutions from an initial cultures of $D^{600}=1$ were plated in SC-URA Glc or Gly-EtOH
795 supplemented with 2mg/l or without (wo) methionine (increasing Met concentration
796 decrease MET25 promoter activity) to test the effect caused by increasing amount of
797 TcCox15.His-GFP on the respiratory capacity of the WT strain.

798

799

800 **Figure 4. The TcCox15 mutants do not exhibit HAS activity in *S. cerevisiae cox15* Δ cells.**

801 (A) Spot growth assay of *cox15* Δ yeast cells transformed with p426.MET25 (vector) or
802 *ScCOX15.HIS* (ScCox15), *TcCOX15.HIS* (TcCox15) and *TcCOX15HxxxA.HIS* mutants (H129A,
803 H206A and H307A). 5 μ L of four serial dilutions from an initial culture of $D^{600}=1$ were
804 plated in solid SC-URA Glc or SC-URA Gly-EtOH and incubated during 5 days at 30 $^{\circ}$ C to test
805 their respiratory capacity. (B) The oxygen consumption rate of the same transformed yeast
806 cells previously grown overnight in SC-URA Glc was measured in 3% glycerol (v/v). Data are
807 expressed as means \pm S.D. of three technical replicates from one experiment
808 representative of three independent biological replicas. (C) Western blot of mitochondrial
809 extracts from the same transformed *cox15* Δ yeast cells, grown in SC-URA Glc.

810

811

812 **Figure 5. The recombinant TcCox15HxxxA mutants impair *T. cruzi* epimastigotes' growth.**

813 Growth curve of epimastigotes transfected with (A) pTcINDEX.*TcCOX15.HIS* (Tc15), (B)
814 pTcINDEX.*TcCOX15H129A.HIS* (H129A), and (C) pTcINDEX.*TcCOX15H307A.HIS* (H307A),
815 without or with the addition of 0.15 µg/ml, 0.25 µg/ml of tetracyclin (0, 0.15 Tet, 0.25 Tet).
816 In all cases the growth of epimastigotes transfected with pTcINDEX (vector), incubated
817 without and with 0.5 µg/ml of tetracycline, was monitored as control. Cells were
818 maintained in mid-log phase by periodic dilutions every two days. Data are expressed as
819 means ± S.D. of three independent biological replicas. (D) Quantification of the effect
820 produced by the presence of recombinant proteins expressed as a percentage of parasite
821 number of induced/non-induced conditions at day 8.

822

823

824 **Figure 6. The recombinant TcCox15HxxxA mutants are detected in the epimastigotes'**

825 **mitochondrion. (A)** Western blot of total cell-free extracts from epimastigotes transfected
826 with pTcINDEX (vector), pTcINDEX.*TcCOX15.HIS* (Tc15), pTcINDEX.*TcCOX15H129A.HIS*
827 (H129A) and pTcINDEX.*TcCOX15H307A.HIS* (H307A) induced with a monodose of 0.05,
828 0.15, or 0.25 µg/ml tetracycline for 3 days, using the following antibodies: anti-TcCox15,
829 anti-His, and anti-tubulin as a loading control. (B) Indirect immunofluorescence assay of *T.*
830 *cruzi* epimastigotes transfected with pTcINDEX (vector), pTcINDEX.*TcCOX15H129A.HIS*
831 (H129A) or pTcINDEX.*TcCOX15H307A.HIS* (H307A), total TcCox15 was detected using anti-
832 TcCox15 and FITC-conjugated anti-rabbit (green) as secondary antibody. DNA was stained
833 with DAPI (blue) and mitochondrion with Mitotracker (MT). DIC, differential interference
834 contrast image. The confocal images are a representative of multiple fields from three
835 different experiments. The colocalization analysis (Red:Green) was performed on H129A
836 (Pearson's correlation coefficient: 0.927, and Manders overlap coefficients: 0.895 and
837 0.924) and H307A (Pearson's correlation coefficient: 0.331, and Manders overlap
838 coefficients: 0.717 and 0.908).

839

840

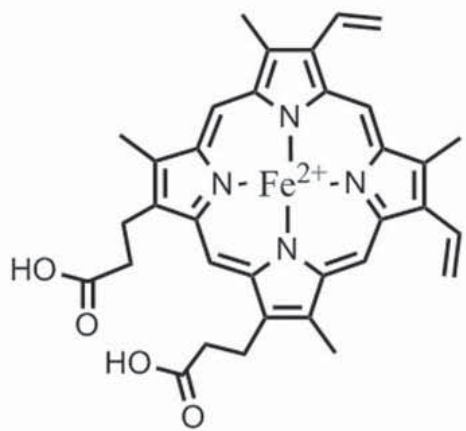
841 **Figure 7. The expression of the recombinant TcCox15H307A protein causes a reduction**
842 **on the oxygen consumption rate in *T. cruzi* epimastigotes.** The oxygen consumption rate
843 (nmoles of consumed O₂/min OD⁶⁰⁰) of epimastigotes transfected with pTcINDEX (vector),
844 pTcINDEX.*TcCOX15.HIS* (Tc15) or pTcINDEX.*TcCOX15H307A.HIS* (H307A) was measured in
845 TSB-EGTA plus 5 mM succinic acid and normalized against parasite number. The
846 transfected epimastigotes were incubated without (non-induced) or with 0.25 µg/ml
847 tetracycline (induced) for 4 days. In each case the oxygen consumption rate was referred
848 to the non-induced condition. Data are expressed as means ± S.D. of three independent
849 biological replicas. Asterisk indicates a statistically significant difference of induced
850 compared to non-induced condition, **P* < 0.01, each case was analyzed by two-tailed
851 paired Student's t test.

852

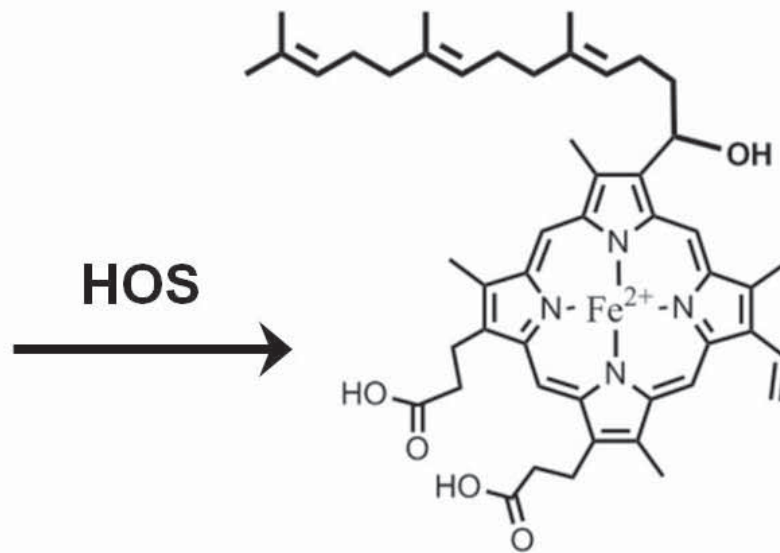
853

854 **Figure 8. The restriction in heme A synthesis (and CcO activity) impairs the**
855 **trypomastigotes' infection and intracellular amastigotes' replication.** To study the effect
856 of a restriction in heme A synthesis and CcO activity on *T. cruzi* infectivity and intracellular
857 replication, the capability of trypomastigotes to infect a cellular line, and intracellular
858 replication of amastigotes were evaluated in the presence of the recombinant
859 TcCox15H307A or TcCox15 proteins during the infection (+/-), post infection (-/+), in both
860 cases (+/+), and compared to control (-/-, without the expression of the recombinant
861 proteins). The infection and post infection incubation were performed in the absence or
862 presence of 0.20 µg/ml of tetracycline: -/- tetracycline never added to the medium; +/-
863 trypomastigotes were pre-treated with tetracycline for 1 h before the infection, it was
864 added only during the infection (16h) and then removed; -/+ trypomastigotes were not
865 induced, tetracycline was added only during 72h after the infection at the amastigote
866 stage; +/+, trypomastigotes were pre-treated and tetracycline was maintained during the
867 whole assay. The cells were stained with Giemsa reagent and the percentage of infected
868 cell (infection capacity) and number of amastigotes per infected cell (intracellular
869 replication) evaluated under light microscope. **(A and D)** The percentage of infected cells
870 is expressed as means ± S.D. of three independent biological replicates and analyzed by

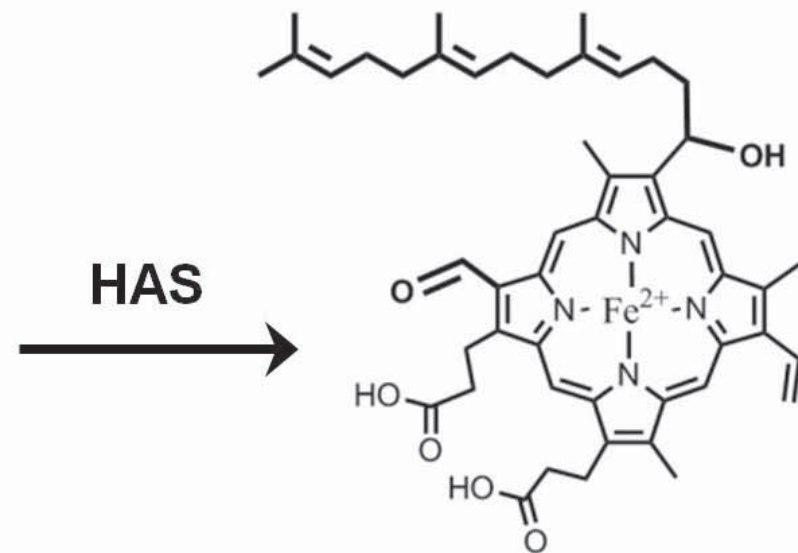
871 One-way analysis of variance followed by Dunnett's Multiple Comparison post-test ($*P <$
872 0.001). (**B** and **E**) The number of intracellular amastigotes per infected cell is shown in a
873 box and whisker plot (the box indicated the first quartil, the median and the third quartil,
874 and the whisker indicated the 5th and 95th percentile), the mean is indicated with a dash,
875 and analyzed by Kruskal-Wallis test followed by Dunn's Multiple Comparison post-test ($**P$
876 < 0.001). (**C** and **F**) Images of Giemsa-satined infected cells. (**G**) Western blot of total cell-
877 free extracts from cell-derived trypomastigotes (T) and amastigotes (A) transfected with
878 pTcINDEX.*TcCOX15.HIS* (Tc15) or pTcINDEX.*TcCOX15H307A.HIS* (H307A) treated with 0.20
879 $\mu\text{g/ml}$ of tetracycline for 0, 1 and 16 h (T) or during 0 and 48h (A), using the following
880 antibodies: anti-TcCox15 and anti-tubulin as a loading control.



Heme B



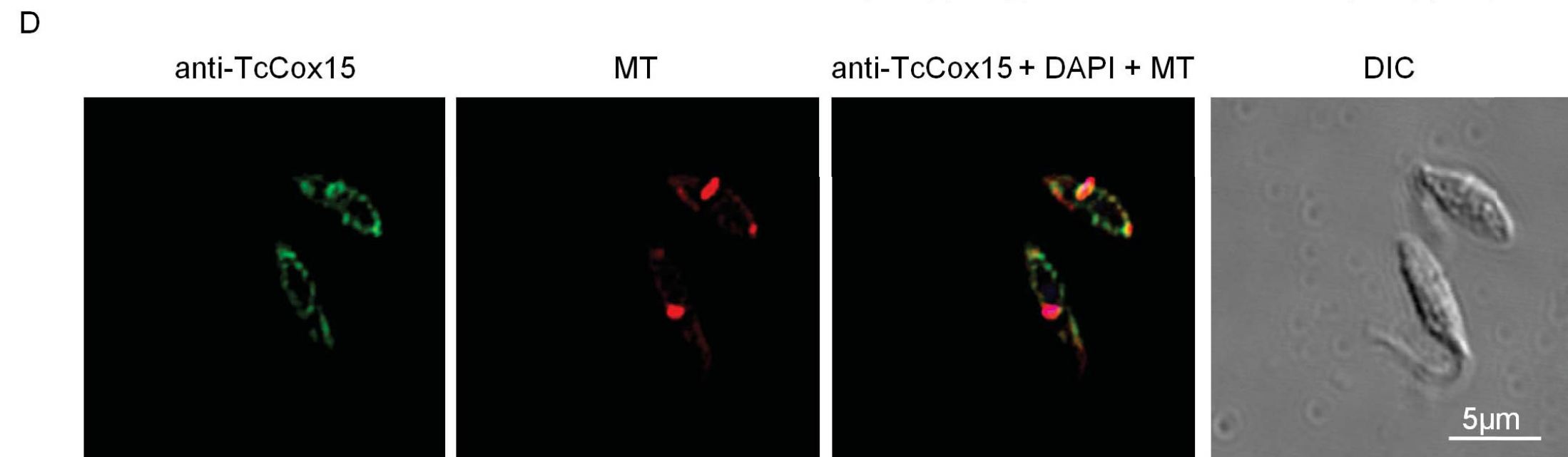
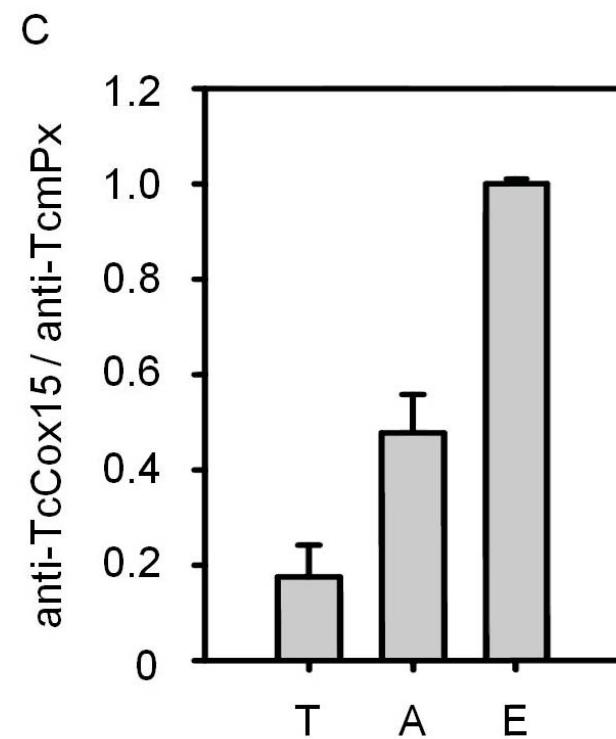
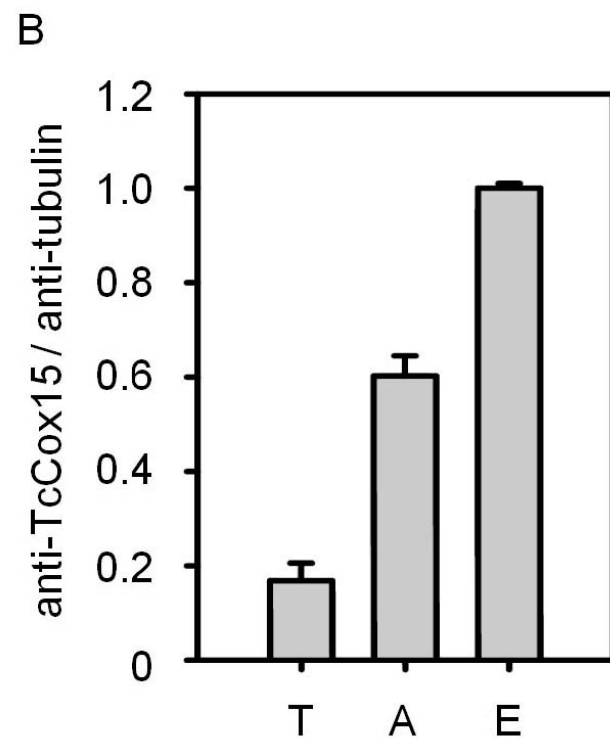
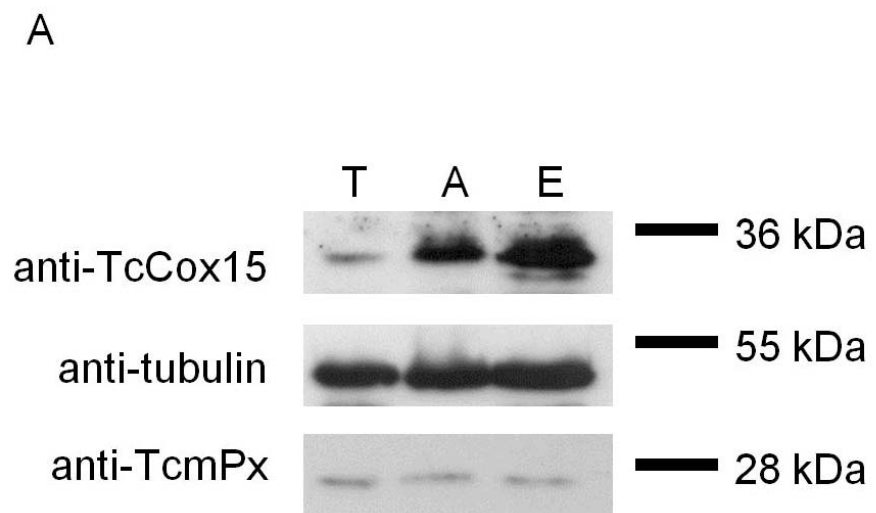
Heme O

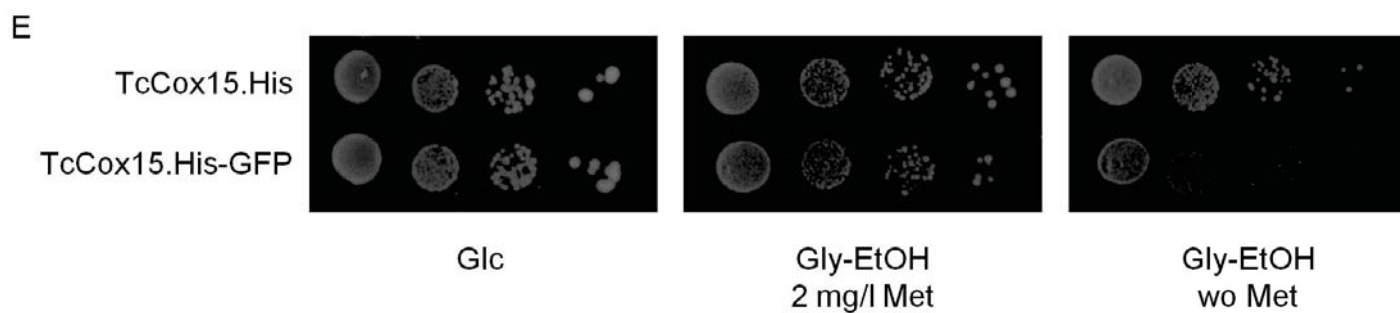
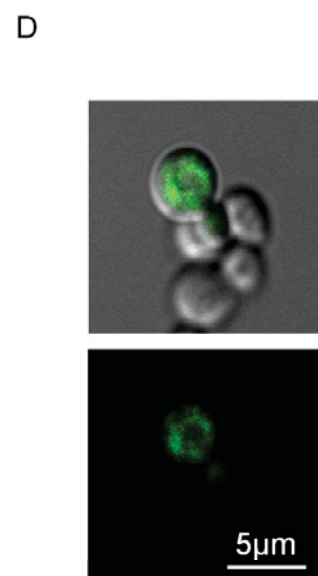
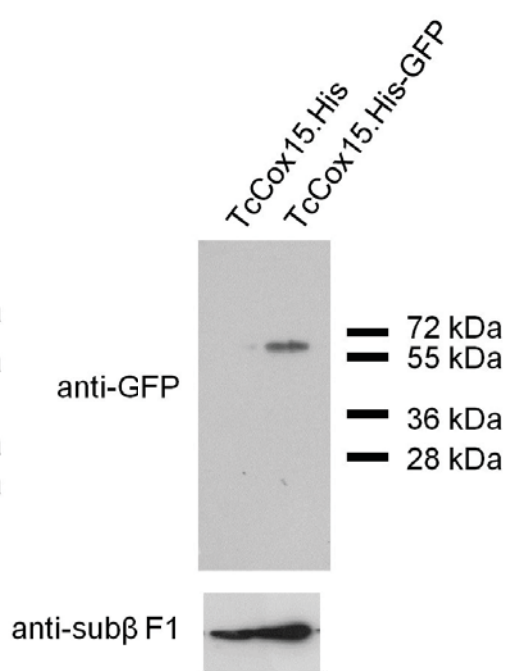
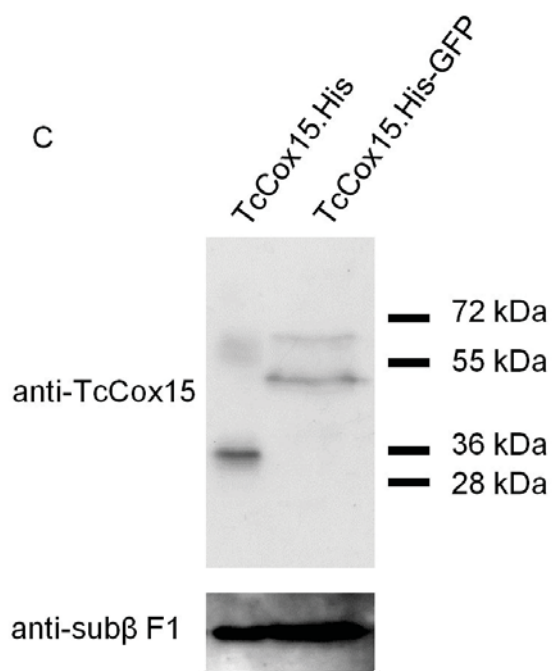
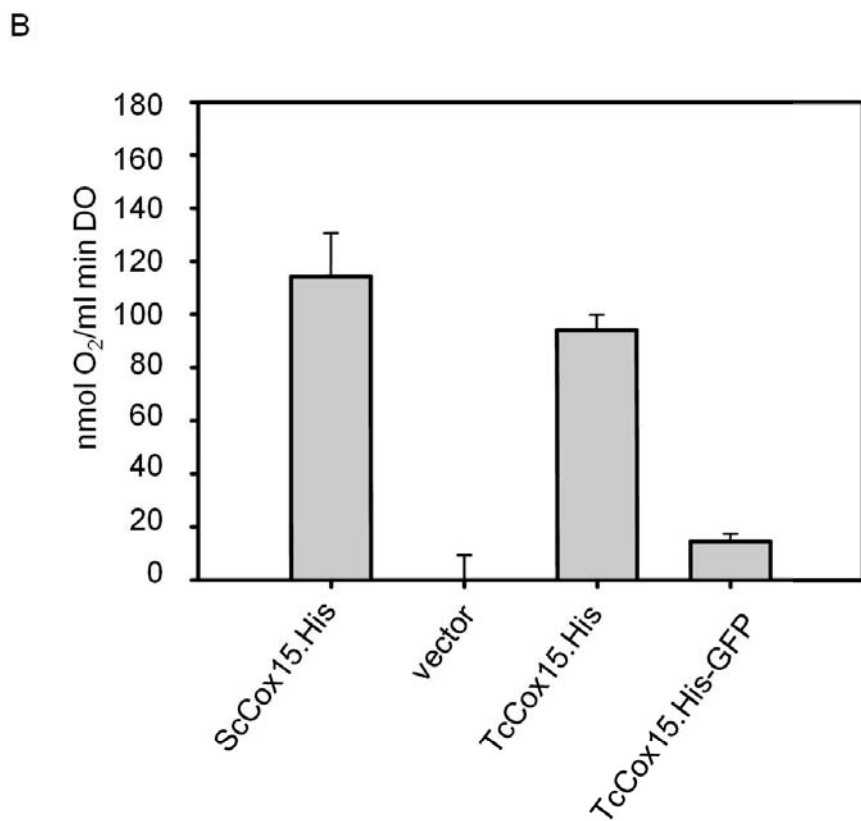
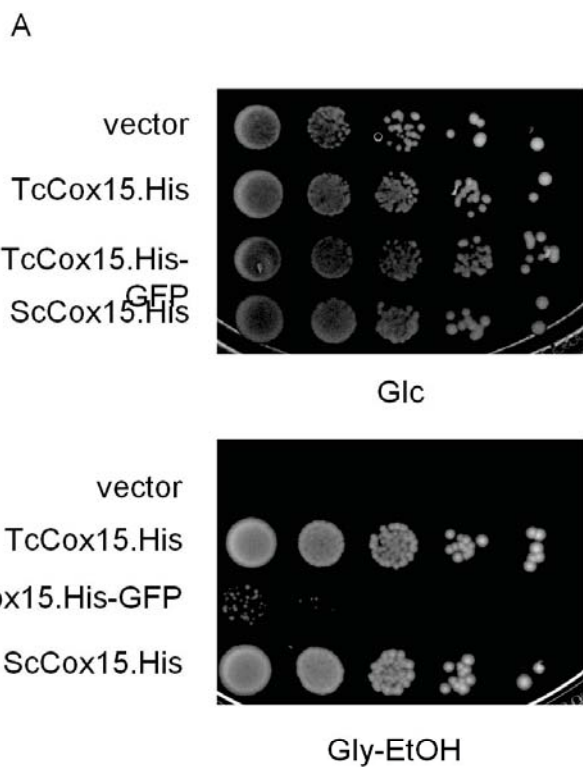


Heme A

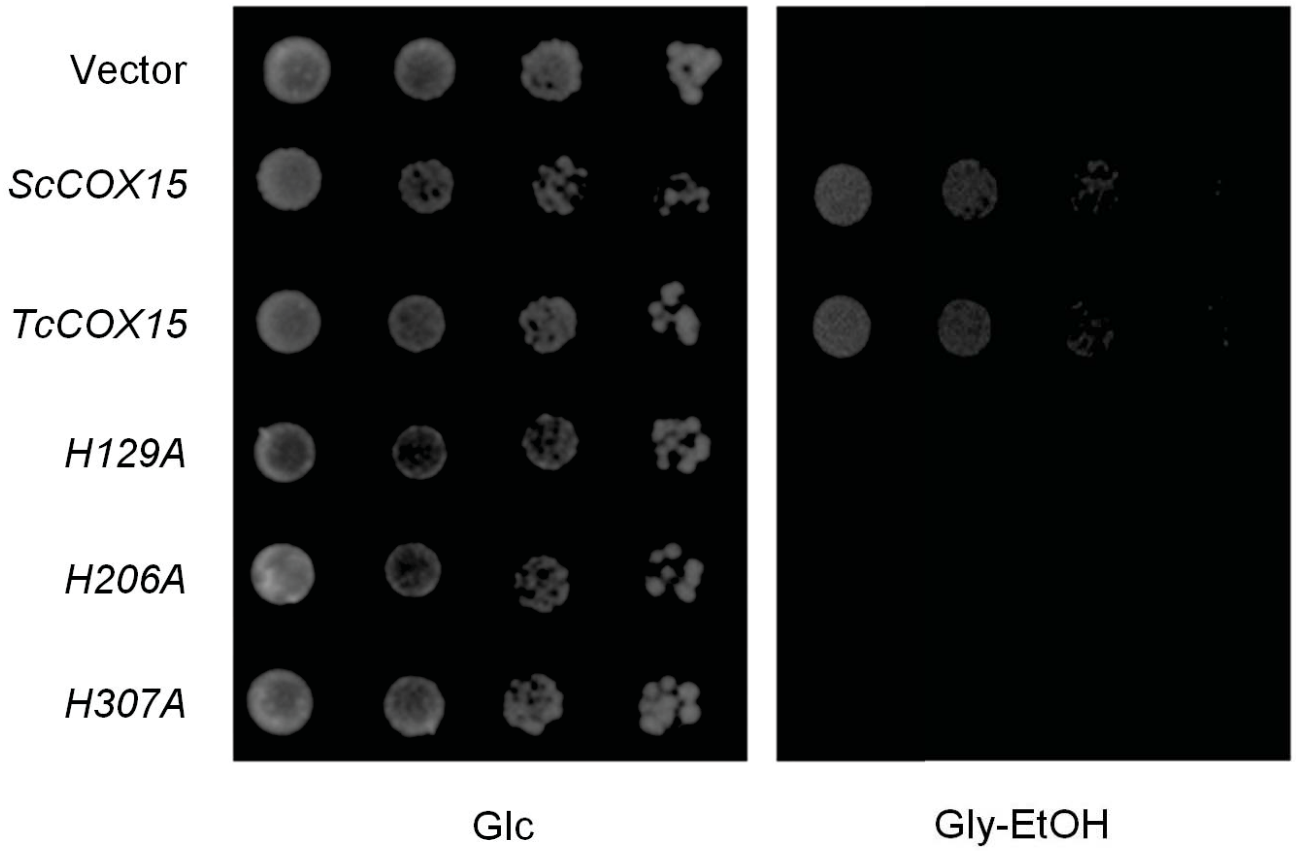
HOS

HAS

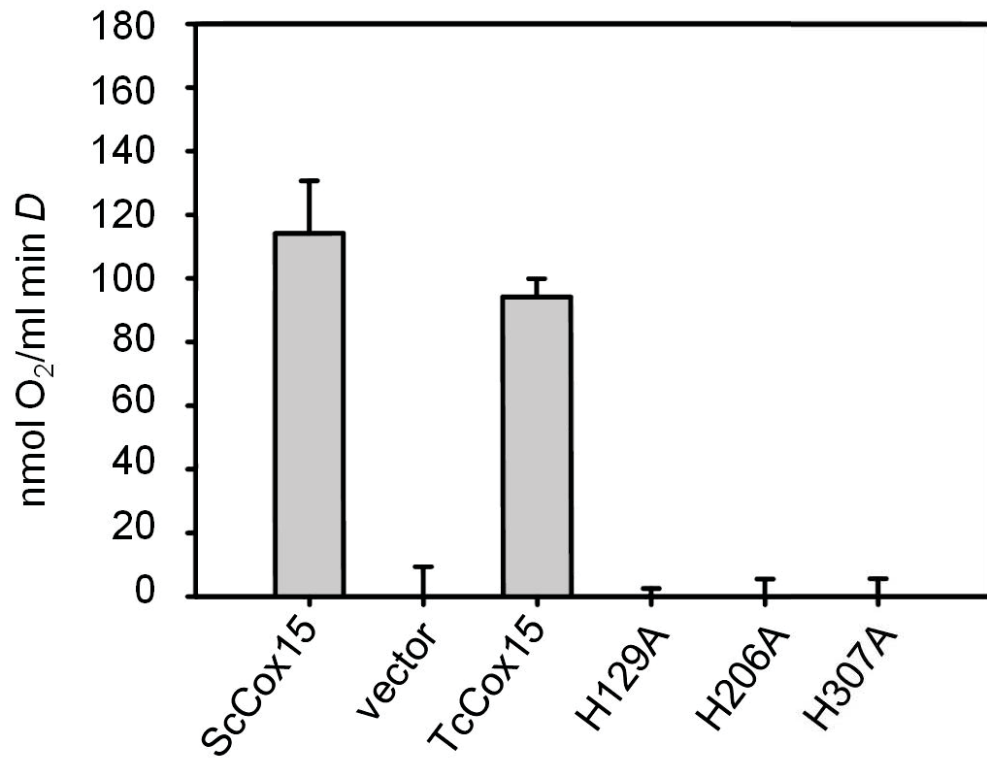




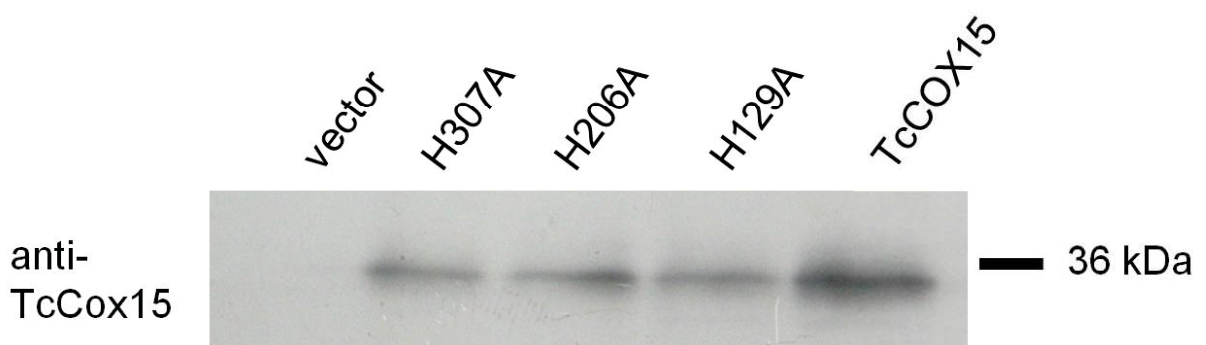
A

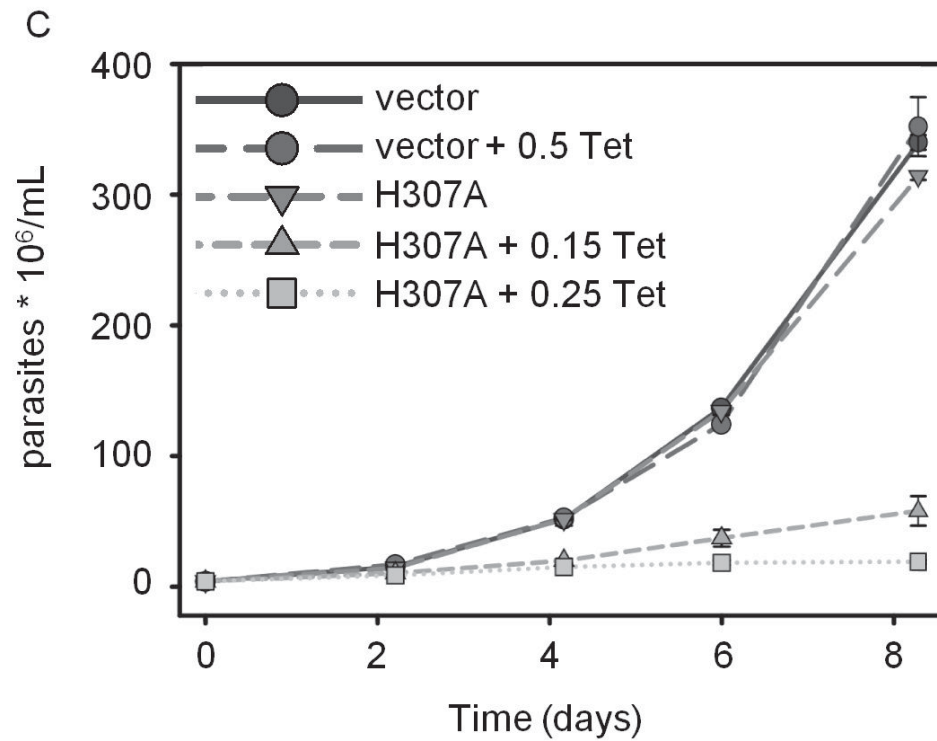
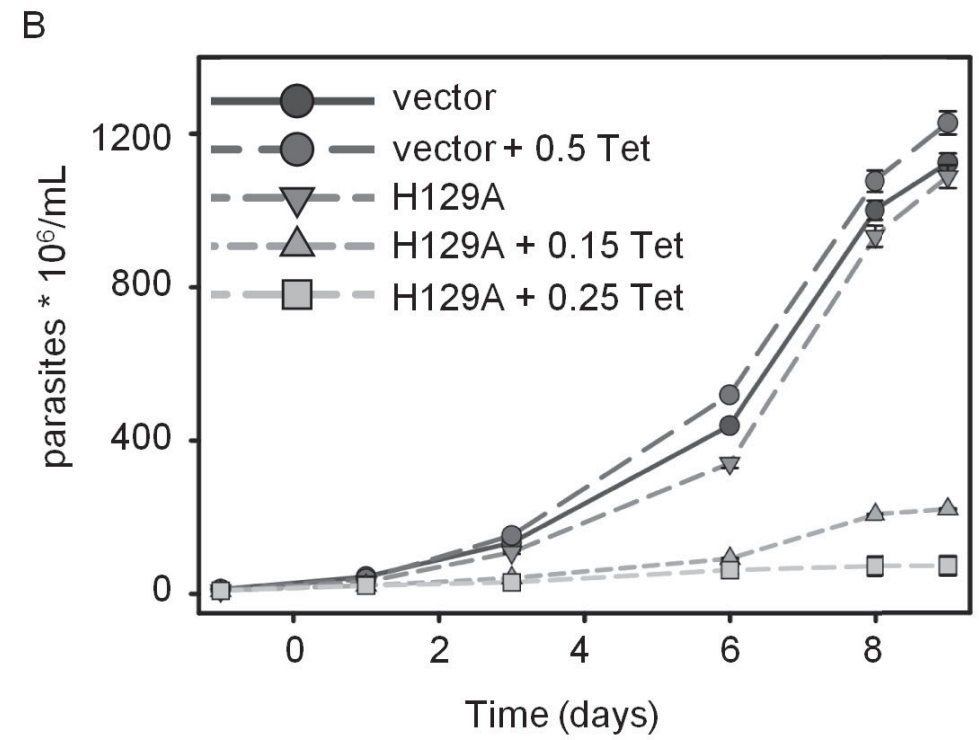
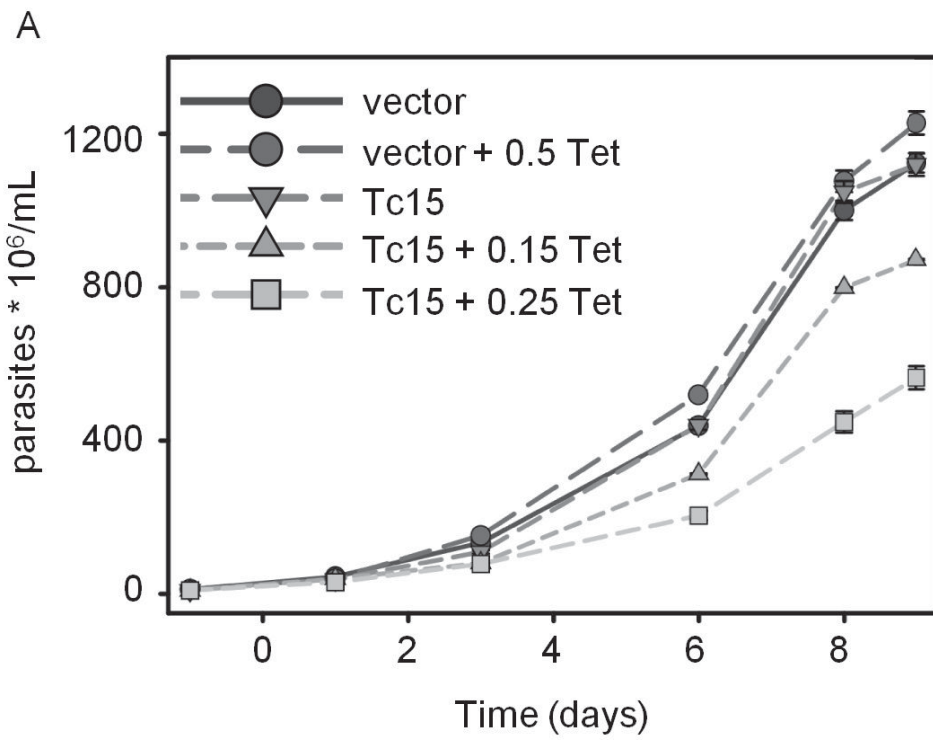


B



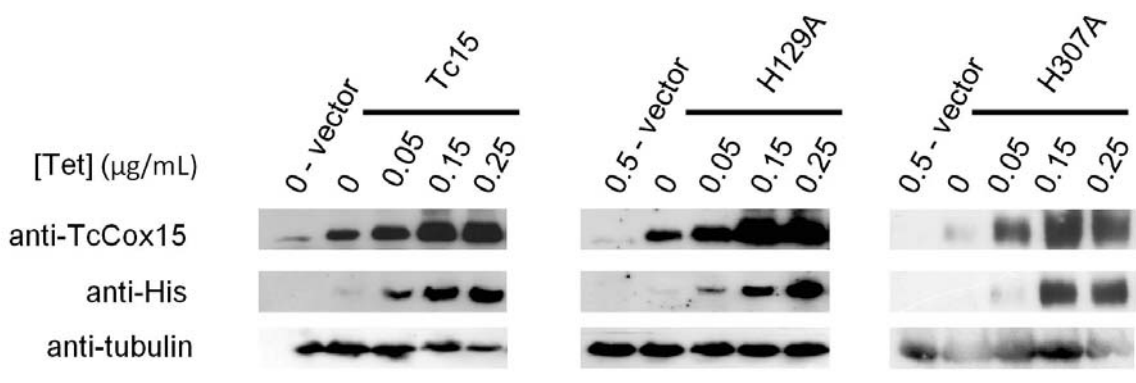
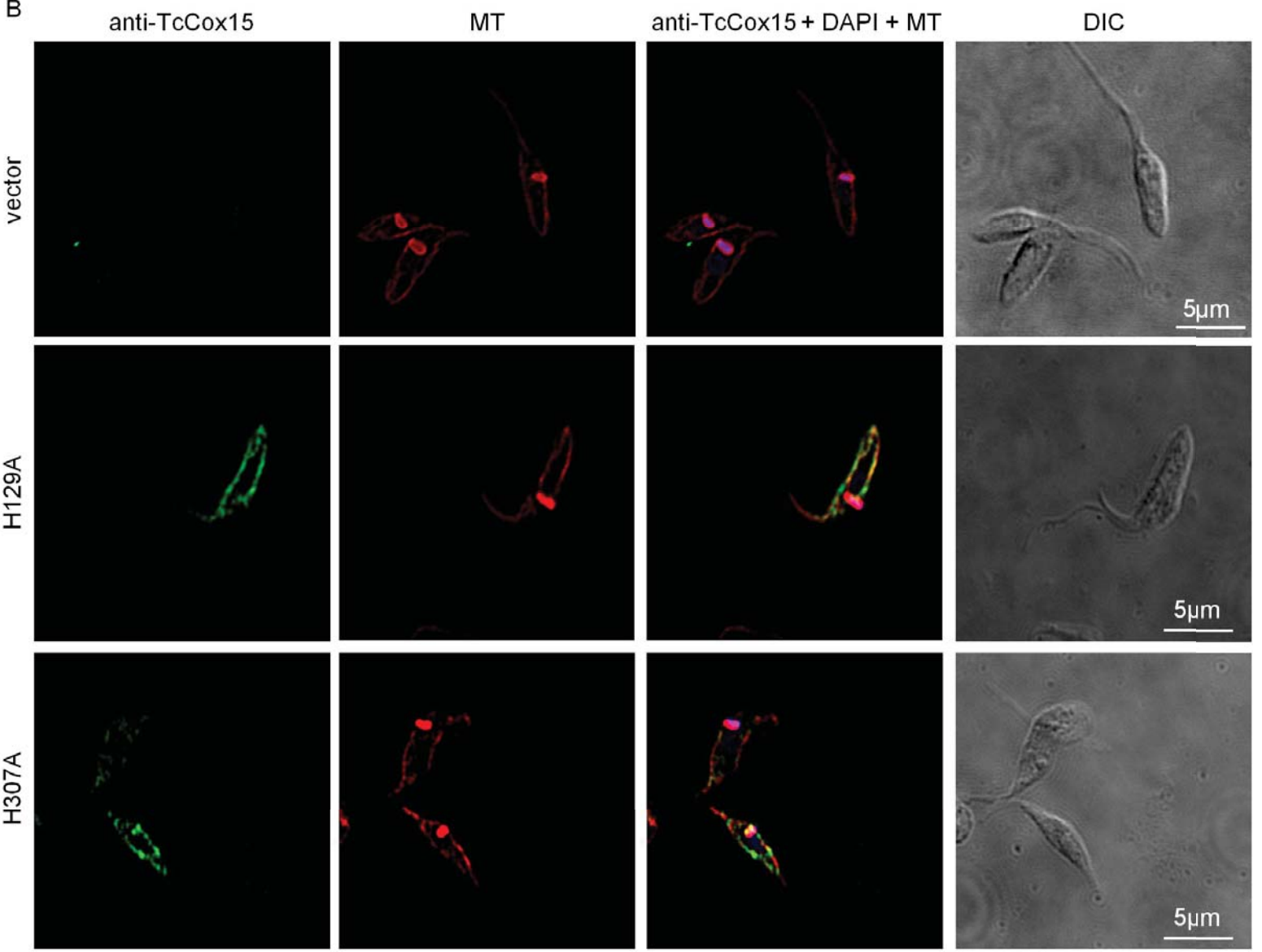
C





D

	% of growth Induced/Non-induced
Tc15 + 0.15 Tet	76.2
Tc15 + 0.25 Tet	42.8
H129A + 0.15 Tet	22.1
H129A + 0.25 Tet	7.7
H307A + 0.15 Tet	18.5
H307A + 0.25 Tet	6.1

A**B**

O₂ consumption ratio
Induced/Non induced

